ISSN 1819-7140, Russian Journal of Pacific Geology, 2009, Vol. 3, No. 1, pp. 40–63. © Pleiades Publishing, Ltd., 2009.
Original Russian Text © I.A. Tararin,V.M. Chubarov, 2009, published in Tikhookeanskaya Geologiya, 2009, Vol. 3, No. 1, pp. 44–65.

Granitization and Magmatic Replacement in the Contact Aureole of the Yurchik Gabbronorite Massif (Ganal Ridge, Kamchatka)

I. A. Tararin[a] and V. M. Chubarov[b]

[a] Far East Geological Institute, Far East Branch, Russian Academy of Sciences, Vladivostok, Russia

[b] Institute of Volcanology and Seismology, Russian Academy of Sciences, Petropavlovsk-Kamchatskii, Russia

Received October 16, 2007

Abstract—It is shown that formation of high-temperature granulite-like rocks in the contact aureole of the Yurchik gabbronorite intrusion of the Ganal Ridge in East Kamchatka was caused by contact metamorphism, metasomatism, and local melting of the primary sedimentary–volcanogenic rocks of the Vakhtalkinskaya Sequence of the Ganal Group. The temperature in the inner part of the aureole reached 700–800°C and caused transformation of basic rocks into two-pyroxene–plagioclase, clinopyroxene–amphibole–plagioclase, and amphibole–plagioclase rocks, while sedimentary rocks were replaced by garnet–biotite and garnet–cordierite–biotite hornfelses. Locally, basic volcanic hornfelses were subjected to metasomatic alteration with the formation of bodies of biotite–orthopyroxene–plagioclase metasomatites. In the zones of the most intense fluid filtration, the metasomatites experienced local magmatic replacement resulting in the formation of biotite–orthopyroxene–plagioclase garnet migmatite veinlets and patches. Bodies of garnet enderbites were formed after sedimentary interlayers at temperatures of 800–800°C and a lithostatic pressure of 3.2–4.8 kbar. The comparison of the chemical composition of the Vakhtalkinskaya basic volcanics and the products of their transformation indicates that, in terms of chemistry, the metasomatic alterations and magmatic replacement correspond to siliceous–alkaline metasomatism (granitization) causing a subsequent and uneven influx of Si, Al, Na, K, Rb, Ba, Zr, Nb, and Cl and removal of Fe, Mg, Mn, Ca, and some scattered elements (Cr, Co, Ti, Y, and S). The processes of metamorphism and metasomatism were presumably provoked by highly mineralized mantle fluids that were filtered through magmatic channels that served as pathways for gabbroid magma.

Key words: hornfels, basic volcanics, metasomatism, magmatic replacement, gabbronorites, Yurchik Massif, Ganal Ridge, Kamchatka.

DOI: 10.1134/S1819714009010047

INTRODUCTION

The discovery of high-temperature granulite-like rocks in the Ganal Ridge in Kamchatka by L.I. Tikhomirov in 1956 opened a long discussion concerning their origin and facies affiliation. Most geologists consider these rocks to be an independent ancient complex of sialic basement of East Kamchatka [3, 5–8, 40], which serves as the base for the formation of all the subsequent deposits. However, other geologists suggest that these metamorphic rocks were formed during contact-reaction processes caused by the intrusion of the Yurchik gabbronorite massif [33, 35, 36, 38, 41].

Our previous works in this region were dedicated to the enderbitization, gabbroization, and magmatic replacement in the contact aureole of the Yurchik gabbronorite massif [33, 35–37]. In this work, new data on the composition of minerals and rocks from the contact zone of the massif with basic volcanic and terrigenous rocks of the Vakhtalkinskaya sequence of the Ganal Group were used to demonstrate the evolution of metasomatism and granitization of hornfels from contact aureole under conditions of a fluid flux.

GEOLOGICAL REVIEW

The Ganal Ridge confined to the Eastern neotectonic uplift of Kamchatka is a half horst gently dipping to the east [28]. Four pre-Eocene structural–compositional complexes (blocks) in tectonic contact were recognized there: the Northern, Stenovoi, Vakhtalkinskii, and Southern [2, 28, 31]. These blocks are considered to have been amalgamated during the Eocene–Early Miocene, when they were tectonically juxtaposed into a single structure and split into individual fragments by sinistral strike-slips and conjugate NW-trending thrusts [18, 31, 39].

The Northern block of the Ganal Ridge is made up of terrigenous–volcanogenic deposits metamorphosed to green-schist facies. The Stenovoi block consists of volcanic and terrigenous–volcanic–siliceous rocks metamorphosed under green-schist and epidote–amphibolite facies conditions. The Southern block comprises greenstone-altered volcanogenic and tuffaceous–terrigenous–siliceous deposits of the Late Cretaceous Irunei Formation [5, 32].

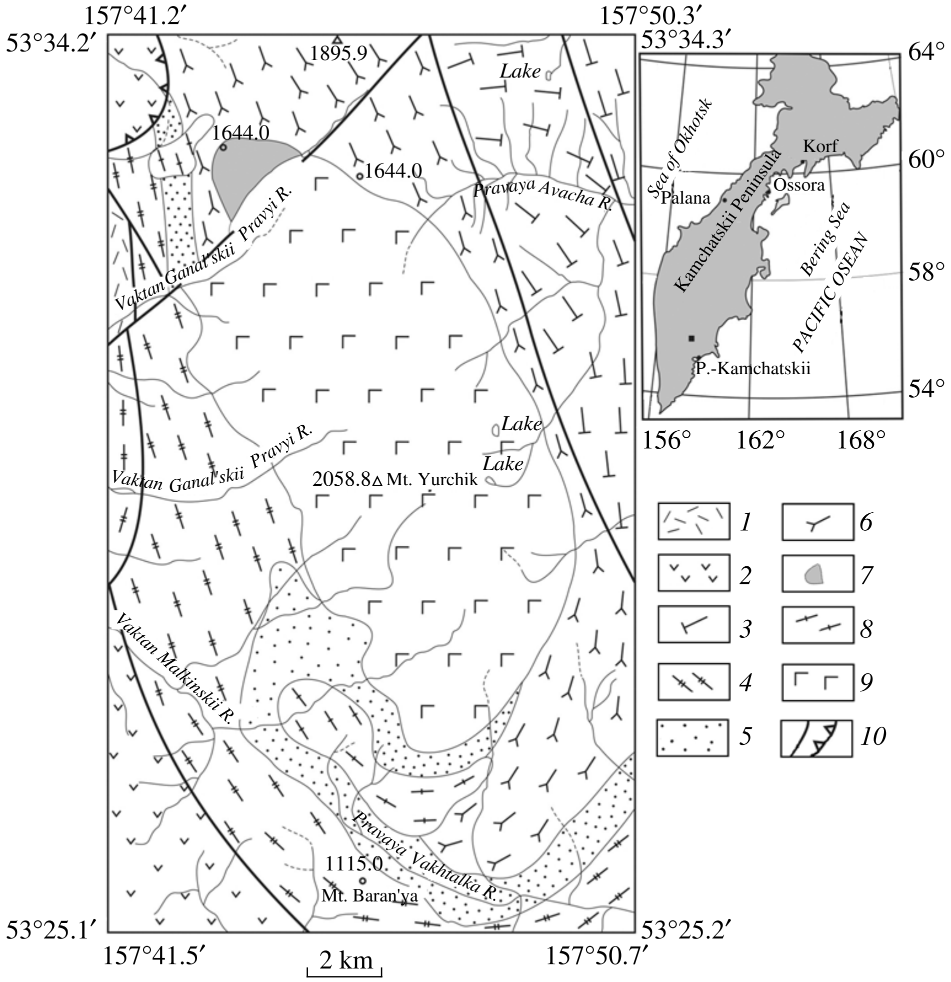

Fig. 1. Schematic geological map of the Vakhtalkinskii block of the Ganal Ridge (compiled using [20]).

(*1*) Neogene tuffs and volcanics; (*2*) Upper Cretaceous (Late Campanian–Maestrichtian) pyroclastic complex of the Irunei Formation; (*3*) terrigenous–volcanic–pyroclastic complex (undivided Stenovaya Group); (*4–6*) terrigenous–volcanogenic complex (Ganal Group): (*4*) terrigenous–volcanogenic (D'yavol'skaya) sequence, (*5*) terrigenous (Voevodskaya) sequence, (*6*) volcanic (Vakhtalkinskaya) sequence; (*7*) zone of intense hornfelsation, metasomatism, and magmatic replacement of the rocks of the Vakhtalkinskaya sequence; (*8*) gneissose amphibole–biotite plagiogranites; (*9*) gneissose metagabbronorites and postmetamorphic clinopyroxene–amphibole gabbro and peridotites of the Yurchik Massif (undivided); (*10*) faults (a), thrusts (b). The black box shows the position of the Yurchik intrusion in the territory of Kamchatka.

The Vakhtalkinskii block demonstrates the most intricate structure (Fig. 1). It consists of four tectonically juxtaposed structural–compositional complexes [31]. The base of the section consists of polymetamorophic rocks of the Ganal Formation, which, from the bottom upward, is subdivided into three units: the Vakhtalkinskaya, Voevodskaya, and D'yavol'skaya [8, 20, 28, 37]. The Vakhtalkinskaya sequence (800–900 m thick) is made up of amphibolites and biotite–amphibole schists intercalated with plagiogneisses, dacitic metavolcanics, quartzites, marbles, and magnetite–garnet–amphibole rocks. The Voevodskaya sequences (800 m) is made up of biotite, garnet–biotite, and garnet–biotite–cordierite plagiogneisses and less common gneisses and their migmatized varieties with thin interlayers of amphibolites, quartzites, and marbles. The D'yavol'skaya sequence (2500–3000 m thick) crowns the Ganal group and consists of alternating amphibolites, and biotite– and garnet–biotite plagiogneisses with scarce intercalations of quartzites and marbles.

The location of the Ganal Group in the lower part of the allochthonous nappes of the Vakhtalkinskii block and the absence of direct geological evidence for the presence of ancient rocks indicate that this group composes the basement of the Ganal Ridge of East Kamchatka. However, according to [25], the fact that the metamorphic rocks of the ridge contain xenogenic zircons with preserved Precambrian signatures keeps open the question of the presence of the Precambrian rocks in the deep-seated parts of the East Kamchatka Precambrian complexes.

The age of the protolith of the Ganal Group and the time of its metamorphism are strongly debatable. The

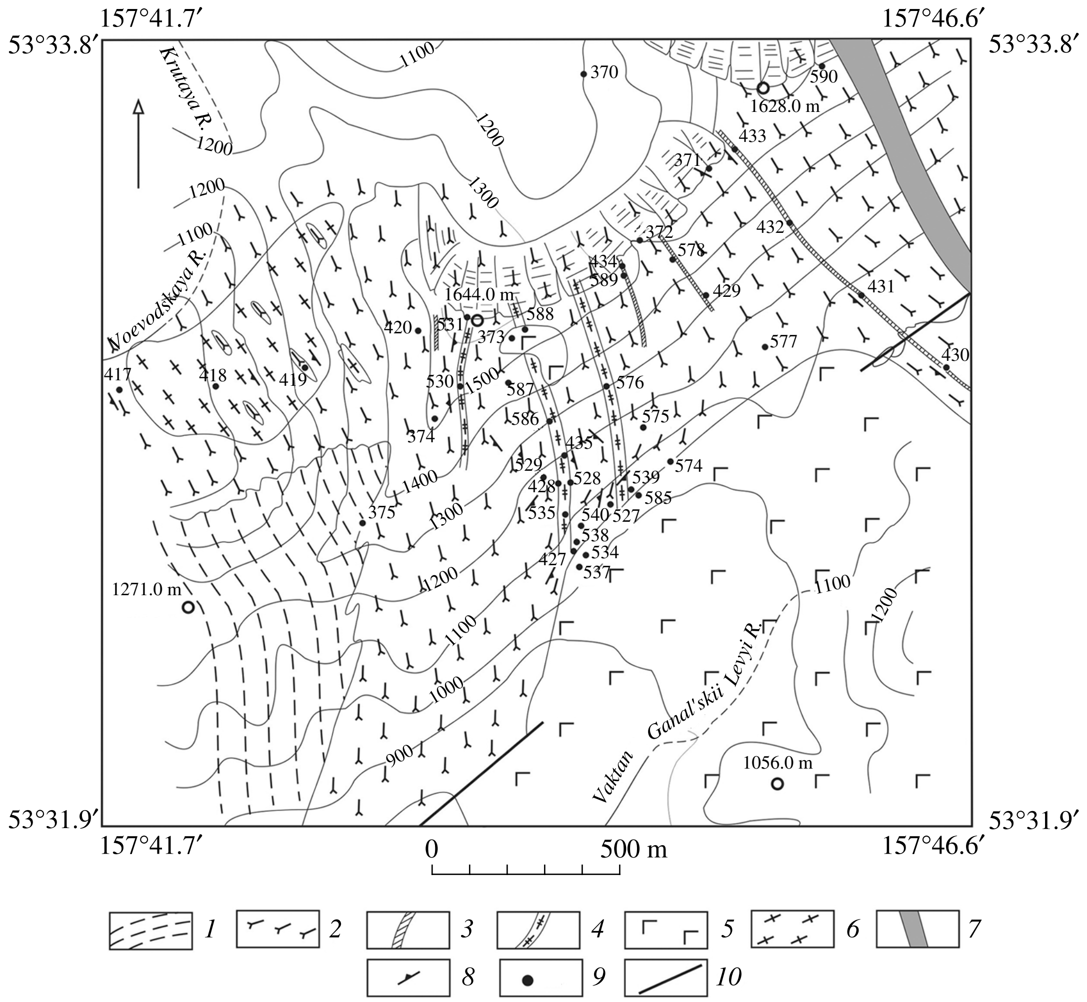

Fig. 2. Structural geological scheme of the contact aureole in the northern part of the Yurchik Intrusion.

(*1–2*) metamorphic rocks of the Ganal Formation: biotite and garnet–biotite plagiogneisses of the Voevodskaya Sequence (*1*), amphibole, clinopyroxene–amphibole, and two-pyroxene–amphibole hornfels after basic volcanics of the Vakhtalkinskaya Sequence, biotite–orthopyroxene–plagioclase metasomatites (*2*); (*3*) intercalations of biotite and garnet–biotite hornfels; (*4*) bodies of garnet enderbites and plagiogneisses; (*5*) gneissose metagabbronorites; (*6*) gneissose amphibole–biotite metaplagiogranites; (*7*) zone of intense pyritization of the intercalated siliceous (dacitic) and basic metavolcanics; (*8*) dip and strike of schistosity, gneissosity, and banding; (*9*) observation points; (*10*) tectonic faults.

age estimates obtained from geological data and K–Ar and Rb–Sr studies yielded very controversial values ranging from Precambrian to Cenozoic [3, 5–8, 38, 45]. ^{40}Ar/^{39}Ar dating showed that the metamorphism age corresponds to the Eocene (47–50 Ma) [19]. The Sm–Nd isochron obtained on whole rock, plagioclase, and ortho- and clinopyroxene from the gabbronorite of the Yurchik intrusion defines an age 27 ± 24 Ma, while data points of whole-rock sample and minerals of high-temperature garnet–orthopyroxene–cordierite–biotite plagiogneiss in the Sm–Nd diagram define the age of metamorphism at 11 ± 19 Ma [25]. U–Pb SHRIMP dating of these plagiogneisses confirm that the metamorphism and emplacement of the gabbronorite of the intrusion occurred in the Late Eocene (about 35 Ma ago) [25].

The Yurchik gabbronorite massif (oval in shape and with area of 50 km^2) occupies the central part in the Vakhtalkinskii block. Geophysical studies showed that the intrusion has a phacolithic shape (up to 22 km along the long axis) and is presently only half eroded. The highest thickness of the intrusion (up to 1500 m) and magmatic conduits were recorded by geophysical methods it its northern part (in the heads of the Vaktan Ganal'skii River), where the thickest cap of the host Vakhtalkinskaya sequence cut by gabbronorite apophyses (Fig. 2, observation points 373, 358) caused intense high-temperature hornfelzation accompanied by metasomatic transformations and magmatic replacement (with debasification and granitization) of primary rocks.

The Yurchik Massif consists of gabbroids of two independent intrusive phases. The rocks of the first phase occupy the most part of the intrusion and comprise gabbronorites with vein facies of hornblende peridotites (cortlandites), fine-grained gabbronorites, and less common pyroxenites. In the marginal zones of the massif, the gabbronorites are strongly gneissose, cataclased, and regionally metamorphosed up to gabbroamphibolites. This superimposed amphibolite-facies metamorphism is concurrent and isofacial with metamorphism of the Ganal rocks, and it caused diaphthoresis of the gabbroids with the formation of migmatite veinlets and hornblendite and amphibole–plagioclase clots [34, 35, 41]. The late (postmetamorphic) gabbroids of the second phase vary in composition from lherzolites, wehrlites, troctolites, and websterites to the prevailing clinopyroxene–amphibole melanocratic gabbro. They are most abundant in the eastern and southern parts of the intrusion, where they form numerous bodies that intrude into the early metagabbronorites and host rocks of the Ganal Group [35, 37, 38]. According to the most recent $^{40}Ar/^{39}ar$ and U–Pb SHRIMP data, the phase 2 gabbroids were intruded at the Oligocene–Miocene boundary (oral communication of E.G. Konnikov).

The metagabbronorites of the Yurchik Massif are made up of plagioclase $An_{45–65}$, clinopyroxene $Wo_{42–46}En_{39–40}Fs_{14–18}$, orthopyroxene $Wo_{1–3}En_{63–65}Fs_{35–38}$, magnesian hornblende (according to the nomenclature [44]), and accessory apatite, ilmenite, magnetite, and Zn-bearing Fe–Al spinel (up to 2–5 wt % ZnO).[1] The major minerals of postmetamorphic clinopyroxene–amphibole gabbros are plagioclase $An_{60–90}$, magnesian hornblende, as well as subordinate Cr-bearing augite $Wo_{37–46}En_{41–47}Fs_{12–16}$, apatite and ore minerals (magnetite, ilmenite, occasional pyrrhotite, chalcopyrite, and pentlandite) [37].

The emplacement of the Yurchik intrusion converted host sedimentary–volcanogenic rocks of the Vakhtalkinskaya sequence into amphibole, clinopyroxene–amphibole, and two-pyroxene–amphibole high-temperature hornfelses. The steep dip (almost vertical) of the intrusive contact defined the insignificant thickness of the high-temperature contact hornfelses (up to a few tens of meters), which reached several hundreds of meters only in the northern part of the intrusion.

The hornfelses are gray and dark gray fine-grained (crystal size no more than 0.5–1.0 mm) banded rocks of granoblastic texture. They consist of 30–60 vol % brownish green magnesian hornblende or high-Fe pargasite (X_{Mg} = 0.60–0.67, Table 1) and plagioclase (X_{An} = 0.80–0.45), as well as clinopyroxene (X_{Mg} = 0.685–0.770) and less common orthopyroxene (X_{Mg} = 0.70–0.72; Table 2, sample 427-D and sample 537-C) in the pyroxene-bearing varieties. The rocks have elevated contents of apatite, titanite, and ore minerals (magnetite, ilmenite, pyrrhotite, and chalcopyrite). Pyroxenes in hornfelses form either individual bands of variable thickness or more often associate with amphibole and plagioclase.

Across the section of the Vakhtalkinskaya sequence, basic metavolcanics contain thin (from 10–20 cm to 2–3, more rarely, up to 10–15 and more meters) intercalations of terrigenous rocks transformed into biotite, garnet-biotite, and garnet–cordierite–biotite±orthopyroxene hornfelses; beyond the contact aureoles, they were transformed into garnet–biotite and garnet–cordierite–biotite plagiogneisses and their migmatized varieties. Their orientation is conformable with the banding of the primary volcanics (Fig. 2). The thickness of the sedimentary interbeds increases upsection towards the contacts of the Voevodskaya sequence, reaching 20–50 m (Fig. 2). The intercalations of terrigenous rocks are strongly boudinaged and dismembered into individual fragments (Fig. 3). Their bodies contain boudinaged fragments of amphibole and clinopyroxene–amphibole±orthopyroxene hornfelses from a few centimeters to a few meters thick.

The middle part of the Vakhtalkinskaya sequence (Fig. 2) contains a 150-m thick zone in which hornfelses after basic metavolcanics are alternated with more siliceous metavolcanics from 10–20 cm to 15–20 m thick. Felsic metavolcanics are light gray banded rocks of dacitic composition. The banding is accentuated by lenslike aggregates of hornblende and chains of almandine–spessartine garnet (X_{Mg} = 0.107, *Alm* 45%, *Prp* 10, Sps 35, *Grs* 10) in the orthoclase–biotite–plagioclase–quartz±orthopyroxene groundmass. The rocks are enriched in pyrite, whose leaching gives a rusty appearance to all the zones, though the total thickness of the felsic rocks is no more than 30% of the entire thickness.

Downsection in the Vakhtalkinskaya sequence, along the watershed range from a height of 1644.0 m in the northeast toward Mount Tumkhan (1895.9 m) and further to the mouths of the Pravaya Avacha River (Fig. 1), with distance from the contact with Yurchik gabbroids, the hornfelses grade into amphibole and biotite–amphibole schists that resulted from regional metamorphism, which spanned the rocks of the Ganal Group (including hornfels of contact aureole) and gabbroids of the intrusion. The regional metamorphism caused intense diaphthoresis of high-temperature hornfelses at the contact aureole and inner contact gabbronorites (up to gabbroamphibolites) with the formation of numerous migmatite veinlets and patches of

[1] The following mineral abbreviations are used in this paper: *Alm*—almandine, *An*—content of anorthite molecules in plagioclase, *Ap*—apatite, *Crd*—cordierite, *Cpx*—clinopyroxene, *En*—enstatite, *Fs*—ferrosilite, *Grt*—garnet, *Grs*—grossular, *Hbl*—amphibole, *Ilm*—ilmenite, *Opx*—orthopyroxene, *Or*—potassium feldspar, *Pl*—plagioclase, *Prp*—pyrope, *Sps*—spessartine, *Spl*—spinel, *Wo*—wollsatonite. (C) core; (r) rim of the crystal. XMg = Mg/(Mg + Fe + Mn), and XAn = Ca/(Ca = Na + K). The analyses were performed using a Camebax microprobe at the Institute of Volcanology and Seismology of the Far East Branch of the Russian Academy of Sciences.

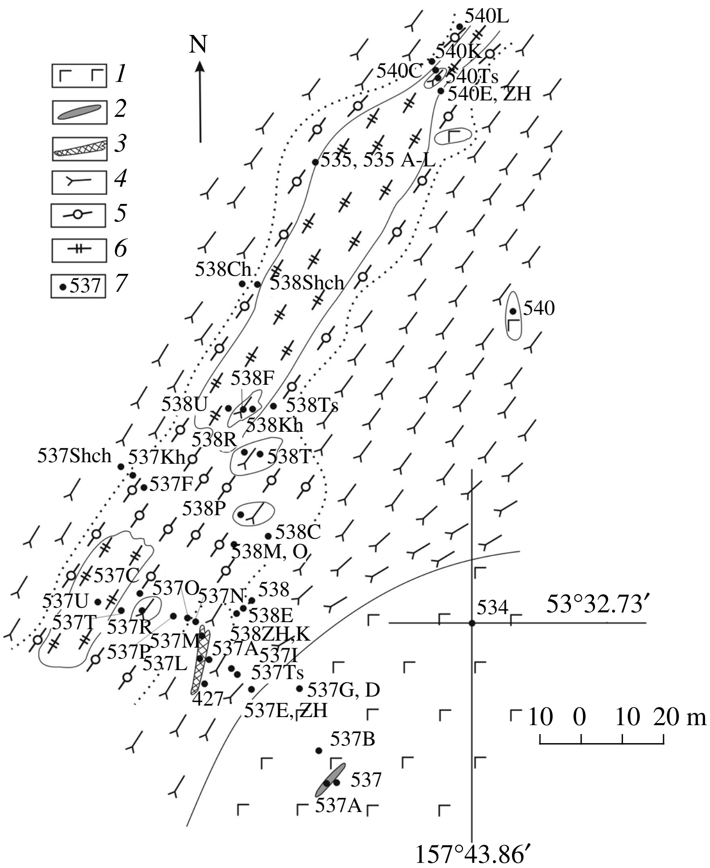

Fig. 3. Zone of metasomatic alteration and magmatic replacement of amphibole and pyroxene–amphibole hornfelses and hornfelsed sedimentary rocks of the Vakhtalkinskaya sequence in the northern part of the contact aureole of the Yurchik gabbroid intrusion (on the southern slope of a 1644.0-m hill). (*1*) gneissose metagabbronorites; (*2*) vein of fine-grained metagabbronorites; (*3*) hornblende orthopyroxenites; (*4*) amphibole and pyroxene–amphibole hornfelses, (*5*) biotite–orthopyroxene–plagioclase metasomatites with migmatite patches and veinlets of biotite–orthopyroxene–plagioclase±garnet composition, (*6*) garnet enderbites and plagiogneisses, (*7*) sampling locality.

hornblendite, amphibole–plagioclase, and plagioclase compositions from a few to a few tens of centimeters thick, which are oriented conformably with the banding or gneissosity of the rocks.

Regionally metamorphosed amphibole schists of the Vakhtalkinskaya sequence (beyond the zone of the contact aureole) contain thin (from a few centimeters to 2–3 m) interlayers of biotite and less common garnet–biotite plagiogneisses, which are significantly less in number as compared to those in the middle and upper parts. Amphibole schists consist of tschermakite or tschermakitic hornblende, plagioclase $An_{32–35}$, magnetite, ilmenite, and often biotite (Table 1, samples 593, 595, 532-A, 533).

METASOMATIC PROCESSES AND MAGMATIC REPLACEMENT

Locally, the hornfelses of the contact aureole suffered alkaline-basic metasomatism, whose intensity was determined by the presence of fracture zones permeable for metasomatic fluids. Metasomatically altered rocks rarely form large exposures; they more often occur as irregularly shaped areas of limited size in the basic volcanic hornfelses of the Vakhtalkinskaya sequence, occasionally amounting to as little as a few tens of cm^2 in area. The largest exposures of metasomatites are restricted to the boudinaged interbeds of siliceous hornfelses after sedimentary rocks (Fig. 3). The boundaries between different lithologies were presumably the most permeable pathways for fluid penetration.

The initial stages of metasomatic transformation of basic hornfels were marked by formation of individual small orthopyroxene crystals (usually with biotite) that corrode and replace hornblende in the initial rocks (Fig. 4). Newly formed orthopyroxene has a higher Fe content as compared to orthopyroxene of hornfelses. Clinopyroxene more rarely forms than orthopyroxene, but it also has a higher Fe composition than the clinopyroxene formed during hornfelsation of basic volcanics (Table 2, sample 427-I).

The intensification of the metasomatic processes leads to almost complete resorption and replacement of all the mafic minerals of hornfelses by a newly formed

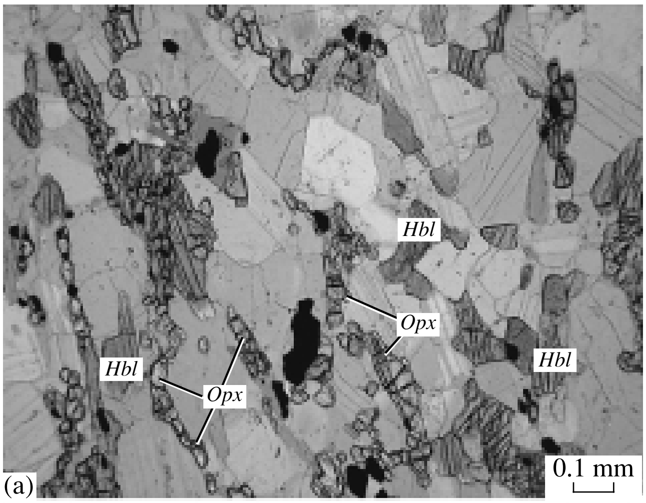

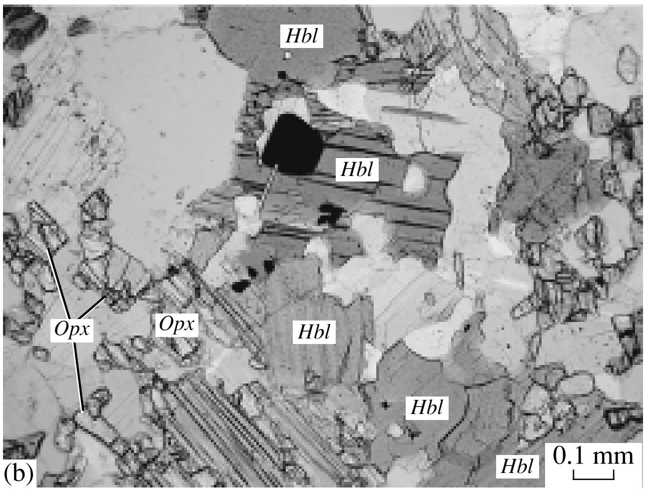

Fig. 4. Metasomatic replacement of the brownish green hornblende by orthopyroxene in basic hornfels.
(a) sample 537-S-1, (b) sample 537-L-1, without analyzer.

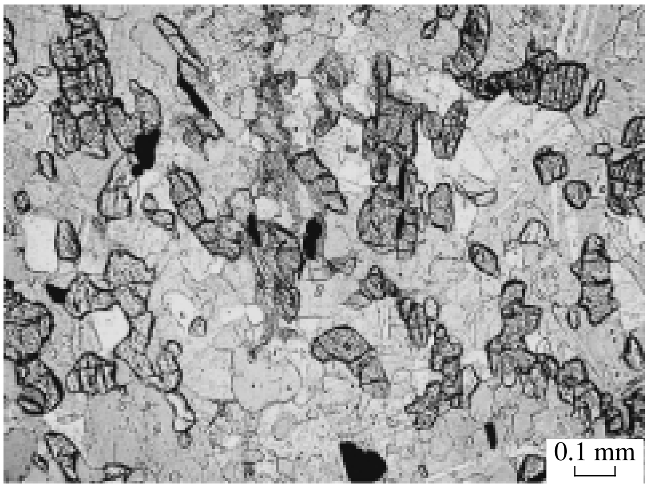

Fig. 5. Fine-grained biotite–orthopyroxene–plagioclase metasomatite. Sample 427-I, without analyzer.

biotite–orthopyroxene–plagioclase assemblage of fine-grained metasomatites (Fig. 5) and formation of thin leucocratic migmatite veinlets, lenses and biotite–orthopyroxene–plagioclase±garnet patches. The formation of biotite in the biotite–orthopyroxene–plagioclase rocks is related to the fluid influx of potassium, thus emphasizing the metasomatic character of the hornfels' replacement.

Metasomatites differ in their dark gray color and consist of orthopyroxene (Table 2) insignificantly varying in composition (X_{Mg} = 0.58–0.63, less common higher Fe varieties have X_{Mg} = 0.45–0.56), plagioclase $An_{40–45}$, and variable amounts of biotite, apatite, and ore minerals.

Leucocratic biotite–orthopyroxene–plagioclase migmatite veinlets, lenses, and patches have hypidiomorphic magmatic textures and consist of large (up to 1–2 and more millimeters) plagioclase crystals $An_{35–50}$ in association with Fe orthopyroxene (X_{Mg} = 0.45–0.67) and biotite (X_{Mg} = 0.45–0.70) (Table 2, Fig. 6). More rarely, these veinlets contain pyrope–almandine garnet (X_{Mg} = 0.166–0.184, Table 2; Sample 427-L, Fig. 7). Biotite–orthopyroxene veinlets can also penetrate into hornfels weakly altered by metasomatic processes (Fig. 8).

Leucocratic biotite–orthopyroxene–plagioclase veinlets and clots similar to leucosome of typical migmatites are formed in the metasomatically altered hornfelses, indicating patch melting (magmatic replacement) of the rocks preliminarily altered by metasomatic processes. The onset of magmatic replacement is marked by the appearance of individual tabular and prismatic orthopyroxene and plagioclase 0.5–1.5 mm in size in fine-grained biotite–orthopyroxene–plagioclase metasomatites (Figs. 9, 10). With increasing amounts, they form lenses, veinlets, and aggregates from tenths of a mm to a few centimeters thick (Fig. 6).

Intensification of metasomatic processes and the appearance of migmatite veinlets and clots in the metasomatically altered hornfelses lead to their debasification and distinct differentiation, which is expressed in the increase of the number of leucocratic migmatite veinlets, biotite–orthopyroxene–plagioclase patches, and plagioclase content at the expense of mafic minerals. In particular, fine-grained biotite–orthopyroxene–plagioclase metasomatite (sample 427-I) contains 28 vol % orthopyroxene, up to 1 vol % biotite, 69 vol % plagioclase, and 2 vol % ore minerals and apatite, while magmatic veinlike aggregates contain 10 vol % orthopyroxene, 5 vol % biotite, 83 vol % plagioclase, and 2 vol % ore mineral and apatite. With increasing amount of plagioclase and a decrease in the An component, K-feldspar antiperthites (up to 1–5 vol %) are formed in the central parts of crystals (Fig. 10). This process is accompanied by increasing Fe mole fraction in mafic minerals and an insignificant increase of the Al content in orthopyroxene, which becomes significant

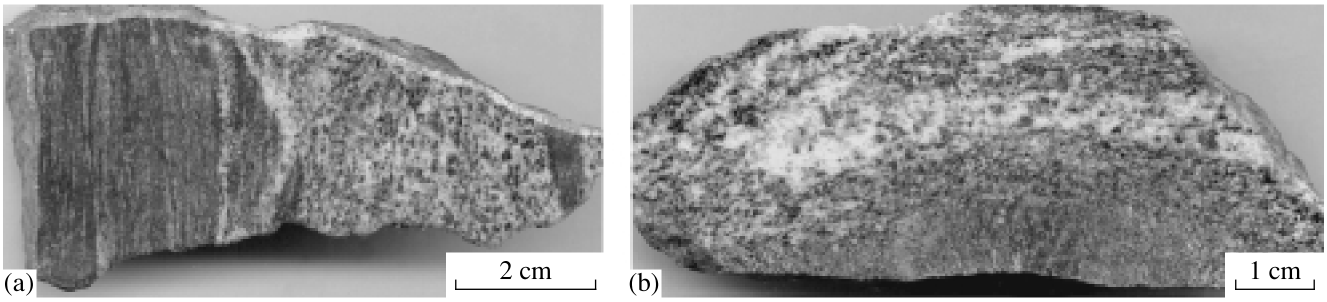

Fig. 6. Leucocratic migmatite biotite–orthopyroxene–plagioclase veinlets and patches in the fine-grained biotite–orthopyroxene–plagioclase metasomatites. (a) sample 535-K, (b) sample 574.

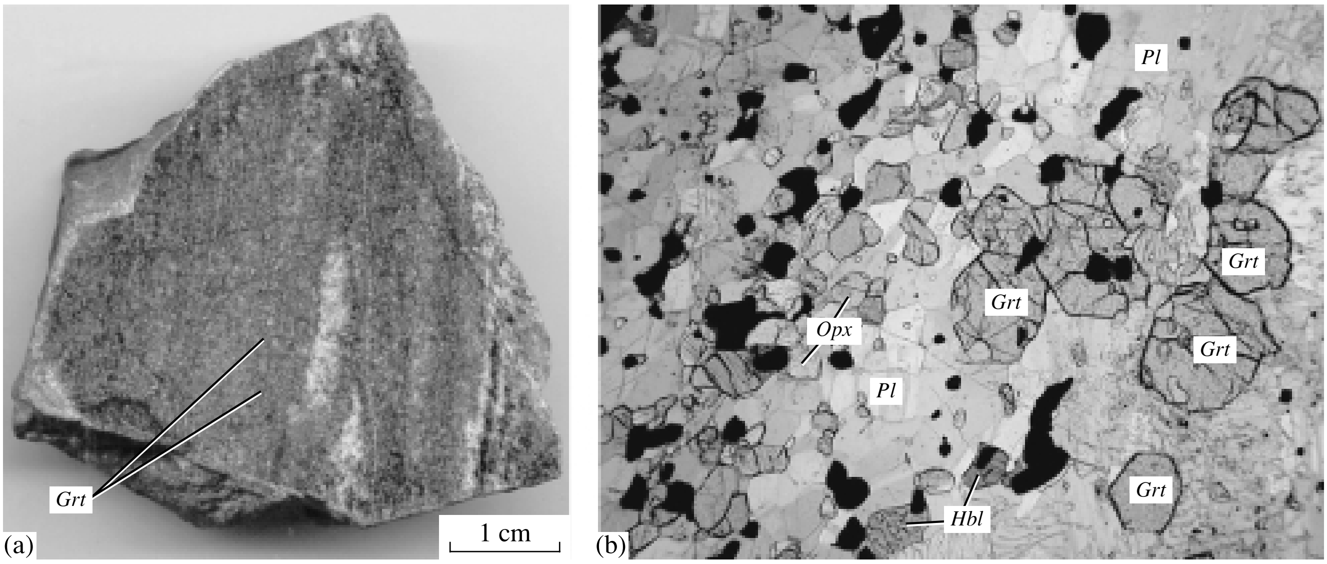

Fig. 7. Vein-like garnet patches in association with orthopyroxene, biotite, and plagioclase in biotite–orthopyroxene–plagioclase metasomatite. (a) sample 427-L; (b) sample 427-N, without analyzer.

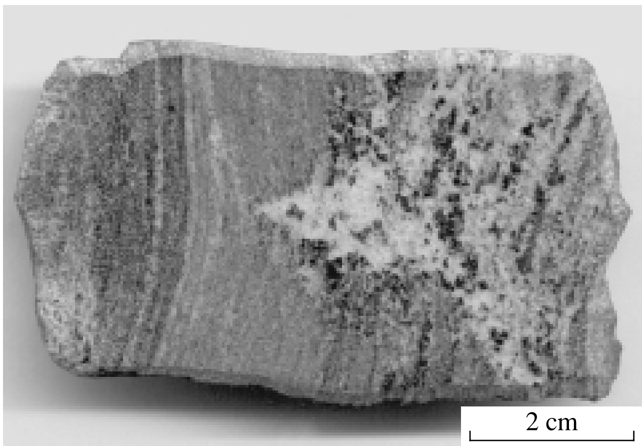

Fig. 8. Intersection of weakly metasomatized amphibole–clinopyroxene–plagioclase basic hornfels by biotite–orthopyroxene–plagioclase veinlets. Sample 537-S.

with the appearance of individual crystals of K–Na feldspar in magmatic melts (Table 2; samples 576, 539-Zh).

The characteristic feature of newly formed migmatite material, as biotite–orthopyroxene–plagioclase metasomatites, is a sharply elevated content of apatite, indicating a high concentration of volatiles (water, phosphorus, chlorine, and fluorine) in the metamorphosing fluids. Magmatic replacement overprinted biotite–orthopyroxene–plagioclase metasomatites, "being superimposed with respect to them as rear zones overprinted frontal zones during the growth of the metasomatic column" [13, p. 51].

The magmatic replacement of sedimentary hornfelses starts from the formation of migmatite veinlets, which, in addition to orthopyroxene, biotite, and plagioclase, contain quartz, garnet, cordierite,and, more rarely, K–N feldspar (Fig. 11). Complete magmatic replacement of sedimentary intercalations (Figs. 2, 3)

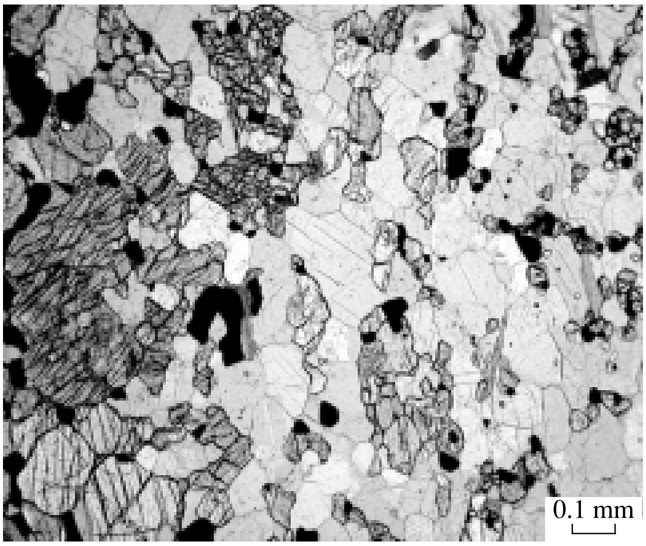

Fig. 9. Chains of orthopyroxenes in fine grained biotite–orthopyroxene–plagioclase metasomatite. Sample 538-Zh, without analyzer.

brings about the formation of large bodies of garnet enderbites and garnet–cordierite–biotite plagiogneisses, which replace garnet enderbites with distance from the contact of the Yurchik Massif. The garnet enderbites contain flattened and equant 5- to 30-cm enclaves of amphibole–plagioclase and more rarely garnet–orthopyroxene–plagioclase hornfelses, which were formed after boudinaged interlayers of basic volcanics. In the marginal parts of the amphibole–plagioclase hornfel enclaves, amphibole is intensely replaced by biotite and orthopyroxene, while Ca plagioclase is replaced by more sodic plagioclase. Some enclaves are rimmed by leucocratic fringes from 0.5–1.0 to 5–10 cm thick (Fig. 12), which consist of cordierite, plagioclase, and quartz and approximate leucocratic rims around melanocratic enclaves in granitoids.

Garnet enderbites are multimineral rocks consisting mainly of plagioclase (40–60 vol %) and quartz (15–25 vol %). Mafic minerals represented by garnet, orthopyroxene, cordierite, and biotite account for, in total, 20–30 vol %. These minerals (representative analyses are listed in Table 3) form a steady assemblage typical of the inner parts of the contact aureole of the Yurchik intrusion.

K–Na feldspar occurs in the metasomatically altered basic hornfelses of aureoles as single antiperthite intergrowths in plagioclase; significant amounts of antiperthites were noted only in garnet enderbites. Individual grains of K–Na feldspar simultaneously form thin veinlets and “films” between plagioclase crystals. The amount of K feldspar in the rock is typically less than 10 vol %, occasionally, for instance, in some hypersthene-bearing veinlets of charnokitoid composition, reaching 50 vol % [36].

Hercynite and sillimanite, the accessory minerals of garnet enderbites, occur together with cordierite, apatite, ilmenite, magnetite and pyrrhotite; pyrite, chalcopyrite, and rutile are less common.

PETROCHEMISTRY AND GEOCHEMISTRY OF THE METASOMATIC AND MAGMATIC REPLACEMENT OF BASIC METAVOLCANICS

The chemical composition of amphibole, amphibole–plagioclase, and pyroxene–amphibole–plagioclase

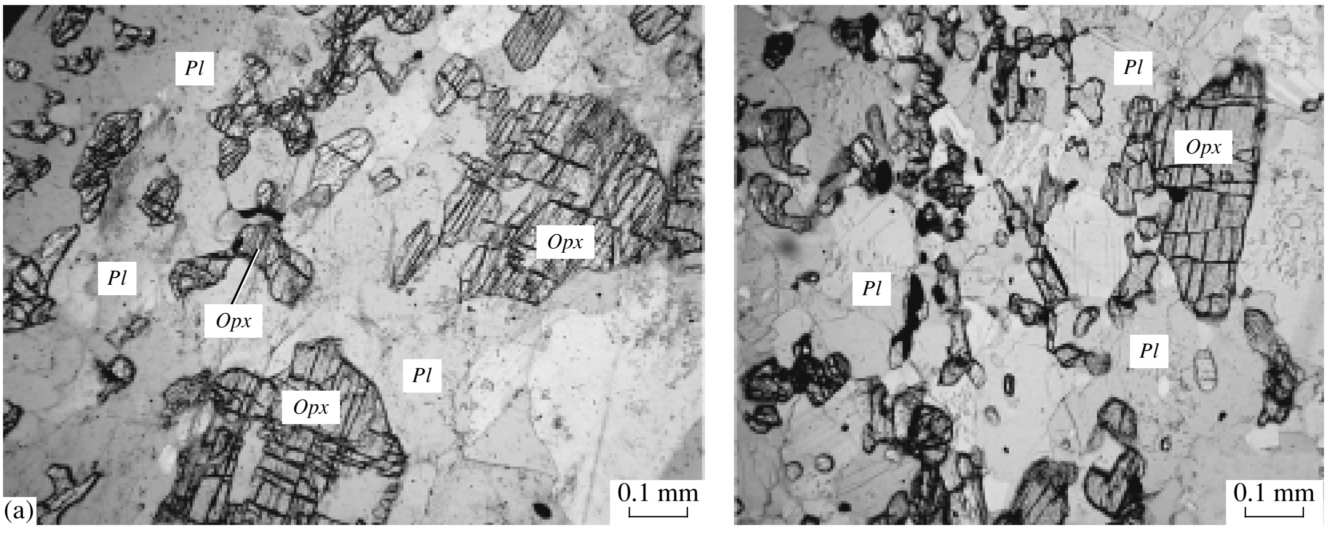

Fig. 10. Biotite–orthopyroxene–plagioclase metasomatites with migmatite veinlets and patches of Bt–Opx–Pl composition. (a) sample 540-L, (b) sample 538-F, without analyzer.

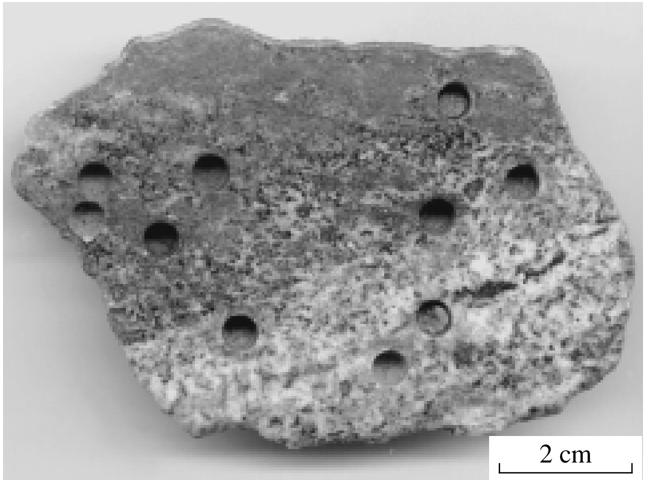

Fig. 11. Migmatite veinlet of garnet enderbite in fine-grained garnet–cordierite–biotite hornfels. Sample 528-I.

Fig. 12. Enclaves of garnet–orthopyroxene–plagioclase hornfels in the garnet enderbite. Sample 535-E.

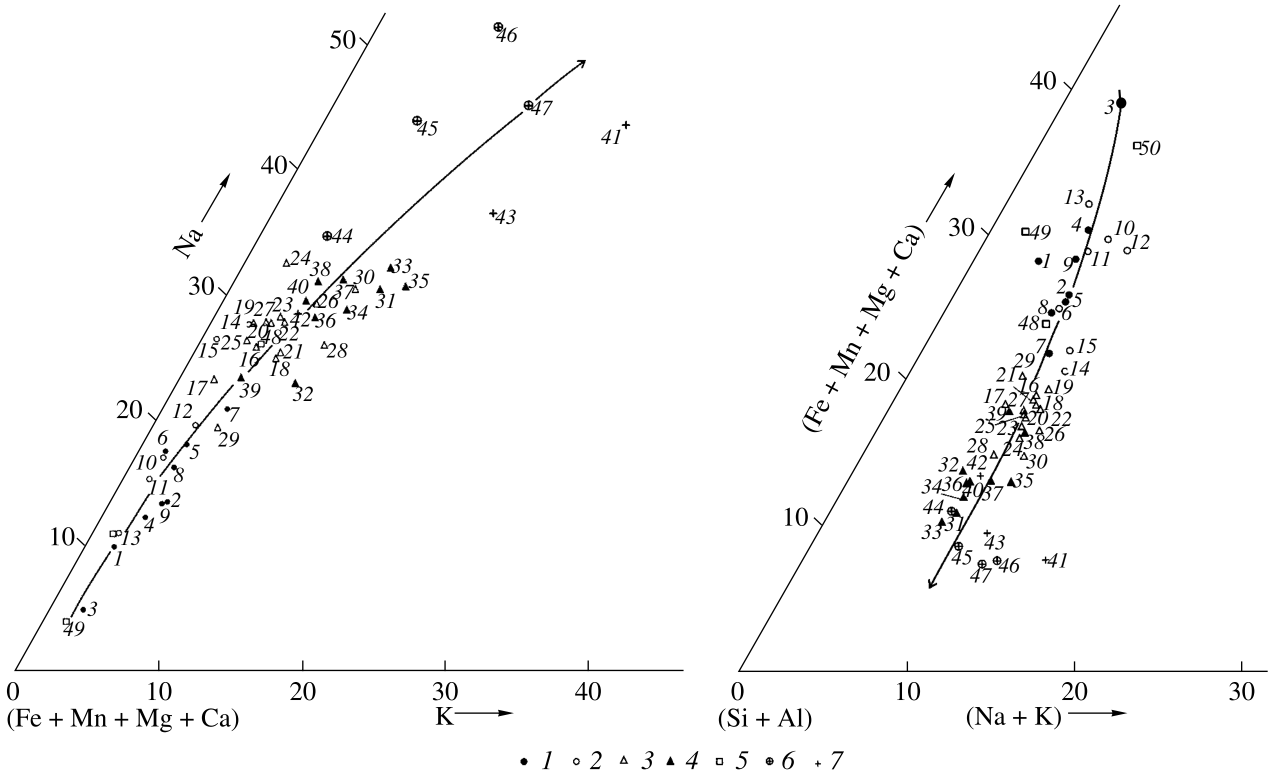

Fig. 13. Petrochemical diagrams illustrating metasomatic alteration and magmatic replacement of basic volcanic and sedimentary hornfelses of the Vakhtalkinskaya sequence in the contact aureole of the Yurchik gabbronorite intrusion.

(*1–2*) metavolcanic hornfels: pyroxene–amphibole–plagioclase (*1*) and amphibole–plagioclase (*2*); (*3*) biotite–orthopyroxene–plagioclase metasomatites; (*4*) garnet enderbites and plagiogneisses; (*5*) xenoliths of basic hornfelses in garnet enderbites; (*6*) charnockitoids; (*7*) metamorphosed silicic volcanic rocks (metadacites). The sample numbers in the diagram correspond to those in Table 4. The arrows show the compositional trend of the metabasic volcanic hornfelses of the Vakhtalkinskaya sequence during granitization and magmatic replacement.

hornfelses, garnet enderbites, and plagiogneisses of the Vakhtalkinskaya Sequences are listed in Table 4. It is seen that primary basites of the Vakhtalkinskaya sequence correspond to basalt having elevated contents of Ti and some trace elements (Sr, Ba, Cr) and lower K contents, which makes them similar to the back-arc

Table 1. Representative microprobe analyses of minerals from amphibole and pyroxene–amphibole hornfelses after basic volcanics of the Vakhtalkinskaya Sequence

Component	Sample 537-I				Sample 427				Sample 427-V				Sample 539		
	Cpx$_r$	*Hbl*$_r$	*Pl*$_r$	Spl	*Cpx*$_r$	*Hbl*$_r$	*Pl*$_r$	*Bt*	*Cpx*$_r$	*Hbl*$_r$	*Pl*$_r$	*Opx*$_r$	*Cpx*$_r$	*Hbl*$_r$	*Pl*$_r$
SiO_2	51.30	41.56	51.58	0.00	52.09	40.04	52.10	36.76	53.13	44.91	50.29	53.02	52.87	44.59	53.16
TiO_2	0.36	2.85	0.00	0.04	0.26	3.21	0.00	4.46	0.03	1.28	0.00	0.00	0.00	1.54	0.00
Al_2O_3	3.06	12.36	30.70	58.04	2.71	12.80	30.47	15.69	1.74	10.74	32.10	1.47	0.78	11.56	29.83
FeO	7.83	13.02	0.31	29.53	7.16	12.38	0.34	13.48	7.53	11.98	0.36	20.87	7.25	11.56	0.47
MnO	0.27	0.20	0.00	1.60	0.27	0.15	0.00	0.09	0.33	0.20	0.00	0.74	0.23	0.23	0.00
MgO	13.09	12.22	0.00	4.60	13.54	10.92	0.00	14.68	14.83	14.06	0.00	23.75	13.88	13.67	0.00
CaO	22.39	11.68	13.13	0.00	23.88	11.86	12.47	0.02	22.38	11.06	14.75	0.32	24.37	10.98	12.32
Na_2O	0.29	1.73	4.11	0.00	0.53	3.31	3.08	0.00	0.17	2.06	3.31	0.00	0.00	1.95	4.41
K_2O	0.00	1.61	0.12	0.00	0.00	1.86	1.41	10.26	0.00	0.35	0.00	0.00	0.00	0.38	0.17
Total	98.59	97.23	99.95	100.03*	100.44	96.53	99.87	95.44	100.14	96.64	100.81	100.17	99.38	96.46	100.36
X_{Mg}	0.742	0.622	–	0.208	0.764	0.608	–	0.658	0.771	0.673	–	0.662	0.768	0.674	–
X_{An}	–	–	0.634	–	–	–	0.632	–	–	–	0.711	–	–	–	0.601
Wo	47.9	–	–	–	49.4	–	–	–	45.8	–	–	0.6	49.4	–	–
En	39.0	–	–	–	39.0	–	–	–	42.2	–	–	66.6	39.1	–	–
Fs	13.1	–	–	–	11.6	–	–	–	12.0	–	–	32.8	11.5	–	–

Component	Sample 539	Sample 539-Ts				Sample 537-L					Sample 537-S				Sample 528-V
	Opx$_r$	*Hbl*$_r$	*Pl*$_r$	*Opx*$_r$	*Bt*	*Cpx*$_r$	*Hbl*$_r$	*Pl*$_r$	*Opx*$_r$	*Bt*	*Cpx*$_r$	*Hbl*$_r$	*Pl*$_r$	*Opx*$_r$	*Cpx*
SiO_2	53.58	43.83	50.43	52.53	36.75	52.28	40.18	48.34	54.74	37.13	52.77	47.19	51.42	54.20	53.33
TiO_2	0.06	1.59	0.00	0.05	2.67	0.11	1.42	0.00	0.02	4.56	0.14	1.01	0.00	0.00	0.03
Al_2O_3	1.60	11.47	31.84	1.59	15.56	1.85	15.12	33.04	1.28	14.51	2.45	9.70	31.77	1.33	1.12
FeO	20.45	11.73	0.32	20.20	17.37	8.86	11.53	0.29	1.48	13.48	7.19	8.81	0.24	16.86	7.74
MnO	0.57	0.26	0.00	0.65	0.40	0.45	0.21	0.00	1.02	0.14	0.95	0.32	0.00	1.24	0.26
MgO	23.42	13.73	0.00	23.69	12.84	13.55	12.70	0.00	21.08	14.95	14.32	15.99	0.00	25.19	13.91
CaO	0.54	11.00	14.54	0.42	0.06	21.92	11.91	15.63	0.49	0.03	21.97	11.32	14.07	0.50	21.88
Na_2O	0.00	2.25	3.15	0.00	0.00	0.39	2.28	2.45	0.43	0.03	0.11	1.22	3.19	0.00	0.03
K_2O	0.00	0.38	0.01	0.00	9.86	0.00	2.57	0.05	0.00	10.07	0.00	1.01	0.18	0.00	0.00
Total	100.22	96.24	100.29	99.13	95.51	99.41	97.92	99.80	100.54	95.16	99.90	96.57	100.87	99.32	98.30
X_{Mg}	0.665	0.671	–	0.669	0.563	0.722	0.658	–	0.625	0.662	0.758	0.757	–	0.712	0.756
X_{An}	–	–	0.718	–	–	–	–	0.777	–	–	–	–	0.705	–	–
Wo	1.1	–	–	0.9	–	46.0	–	–	1.0	–	46.3	–	–	1.0	46.3
En	66.4	–	–	67.0	–	39.5	–	–	63.0	–	41.9	–	–	72.0	40.9
Fs	32.5	–	–	32.1	–	14.5	–	–	36.0	–	11.8	–	–	27.0	12.8

Table 1. (Contd.)

Component	Sample 528-V					Sample 595			Sample 593		Sample 533		Sample 532-A	
	Hbl$_r$	*Pl*[1]	*Pl*[2]	*Opx*$_r$	*Bt*	*Hbl*$_r$	*Pl*$_r$	*Bt*	*Opx*$_r$	*Bt*	*Cpx*$_r$	*Hbl*$_r$	*Pl*$_r$	*Opx*$_r$
SiO_2	46.45	57.17	58.38	53.38	38.37	43.24	60.70	37.45	43.33	60.62	44.56	60.22	44.04	57.12
TiO_2	1.53	0.00	0.00	0.05	3.96	0.38	0.00	1.55	0.37	0.00	0.27	0.00	0.29	0.00
Al_2O_3	9.99	27.11	27.27	1.59	14.27	13.72	24.85	16.96	14.20	25.00	13.72	24.13	14.50	27.29
FeO	9.89	0.38	0.26	21.10	12.67	16.62	0.29	16.05	16.42	0.20	15.34	0.37	16.28	0.20
MnO	0.17	0.00	0.00	0.91	0.08	0.16	0.00	0.00	0.45	0.00	0.29	0.00	0.35	0.00
MgO	14.07	0.00	0.00	22.64	16.02	11.56	0.00	15.13	11.08	0.00	11.41	0.00	10.15	0.00
CaO	10.88	9.16	9.68	0.68	0.08	10.63	6.30	0.02	10.81	6.47	10.91	6.55	11.14	9.09
Na_2O	1.27	6.57	6.05	0.00	0.00	1.74	8.03	0.00	1.86	7.93	1.73	7.89	1.60	6.41
K_2O	0.78	0.07	0.36	0.00	10.18	0.42	0.13	9.48	0.31	0.05	0.26	0.05	0.33	0.07
Total	95.03	100.46	100.00	100.35	95.63	98.47	100.30	96.64	99.33	100.27	98.49	99.21	98.68	100.18
X_{Mg}	0.714	–	–	0.647	0.691	0.551	–	0.627	0.532	–	0.566	–	0.521	–
X_{An}	–	0.434	0.460	–	–	–	0.300	–	–	0.310	–	0.304	–	0.438
Wo	–	–	–	1.4	–	–	–	–	–	–	–	–	–	–
En	–	–	–	64.7	–	–	–	–	–	–	–	–	–	–
Fs	–	–	–	33.9	–	–	–	–	–	–	–	–	–	–

Notes: * the total also includes 0.83 wt % Cr_2O_3 and 5.39 wt % ZnO.

basalts, though some geologists [28, 32] ascribe them to oceanic tholeiites.

The comparison of the chemical composition of basic hornfelses from contact aureole and their alteration products (Tables 4, 5; Fig. 13) indicates that the processes of metasomatism and local melting correspond to siliceous–alkaline metasomatism (granitization), which is accompanied by a subsequent but uneven influx of Si, Al, Na, K, Rb, Ba, Zr, Nb, and Cl and removal of Fe, Mg, Mn, Ca, and some trace components (Cr, Co, Ti, Y, Sc). As is seen in the petrochemical diagrams (Fig. 13), the metasomatic rocks are significantly higher in Si, Na, and K than the primary basic volcanic hornfelses, while the Ba content increases by as much as 5–10 times reaching 10000–1500 g/t (Table 5).

THERMODYNAMIC CONDITIONS OF METAMORPHISM

Intense metasomatism and local magmatic replacement, as well as superimposed amphibolite-facies regional metamorphism, almost completely obscured the hornfels assemblages in the high-temperature aureole of the Yurchik intrusion. The temperature of the contact metamorphism estimated from relict assemblages of magnesian clinopyroxene and orthopyroxene with calcic plagioclase using the Cpx–Opx mineral equilibrium [46] reached 700–800°C (Table 2, samples 427-D, 537-C).

The temperature of the metasomatic alterations of basic hornfels is difficult to determine owing to the absence of precision mineral geothermometers; however, undoubtedly, these processes operated in the same temperature interval as the formation of hornfelses of contact aureole. A similar temperature regime is typical of the local melting of the metasomatically altered hornfelses and formation of biotite–orthopyroxene–plagioclase migmatite veinlets and patches.

The thermodynamic conditions of the formation of garnet enderbites were determined from internally consistent geobarometers [1] at 700–800°C and a pressure of 3.2–4.8 kbar (Table 3), which correspond to a depth about 12–17 km.

DISCUSSION

The geological studies showed that high-temperature granulite-like metamorphic rocks in the Ganal Ridge are of limited abundance and occur only in the

Table 2. Representative microprobe analyses of minerals from basic hornfels, biotite–orthopyroxene–plagioclase metasomatites, and leucocratic migmatite veinlets and patches

Component	Sample 427-D								Sample 427-I						
	Cpx–Pl hornfels		Metasomatically altered *Cpx–Opx–Pl* hornfels			*Bt–Opx–Pl* metasomatite			*Bt–Cpx–Opx–Hbl–Pl* metasomatite						*Bt–Cpx–Opx–Pl* migmatite veinlet
	Cpx_r	Pl_r	Opx_r	Cpx_r	Pl_r	Opx_r	*Bt*	Pl_r	Cpx_r	Opx_r	*Hbl*	*Bt*	*Pl*[1]	*Pl*[2]	Cpx_r
SiO_2	51.49	47.01	53.73	50.80	55.00	53.36	37.86	57.03	51.19	51.73	45.23	35.44	49.87	55.83	50.95
TiO_2	0.09	0.00	0.00	0.17	0.00	0.01	3.94	0.00	0.04	0.09	0.74	3.52	0.00	0.00	0.02
Al_2O_3	1.91	33.59	1.08	2.21	28.73	1.14	14.30	26.98	1.29	0.73	8.86	15.46	31.87	28.24	1.34
FeO	7.53	0.86	17.54	7.91	0.25	18.02	11.28	0.23	13.27	31.40	16.76	20.06	0.20	0.41	14.25
MnO	0.38	0.00	0.97	0.35	0.00	0.95	0.01	0.00	0.43	0.95	0.19	0.11	0.00	0.00	0.34
MgO	14.71	0.00	25.49	14.66	0.00	25.41	17.51	0.00	10.98	15.33	11.10	10.48	0.00	0.00	10.86
CaO	22.19	16.33	0.68	21.37	10.26	0.73	0.29	9.03	21.53	0.98	10.97	0.18	14.36	9.71	20.93
Na_2O	0.56	2.35	0.00	0.53	5.62	0.00	0.02	5.41	0.00	0.00	0.54	0.00	2.94	6.49	0.00
K_2O	0.21	0.28	0.23	0.17	0.64	0.17	9.99	0.57	0.00	0.00	0.81	8.78	0.15	0.28	0.00
Total	99.07	100.42	99.72	98.17	100.50	99.79	95.20	99.25	98.78[1]	101.21	95.65[2]	94.14[3]	99.39	100.96	98.69
X_{Mg}	0.768	–	0.710	0.760	–	0.705	0.734	–	0.588	0.458	0.539	0.481	–	–	0.570
X_{An}	–	0.781	–	–	0.484	–	–	0.463	–	–	–	–	0.723	0.446	–
Wo	45.7	–	1.4	44.6	–	1.5	–	–	45.7	2.1	–	–	–	–	44.4
En	42.2	–	71.1	42.5	–	70.5	–	–	32.4	45.6	–	–	–	–	32.0
Fs	12.1	–	27.5	12.9	–	28.0	–	–	21.9	52.3	–	–	–	–	23.6
T, °C			804 (*Cpx–Opx*)						700 (*Cpx–Opx*)						700 (*Cpx–Opx*)

Component	Sample 427-I				Sample 427-N										
	Bt–Cpx–Opx–Pl migmatite veinlet				*Hbl–Pl* hornfels			*Bt–Opx–Pl* metasomatite				*Bt–Hbl–Opx–Pl* migmatite veinlet			
	Opx_r	*Bt*	*Pl*[1]	*Pl*[2]	Hbl_r	*Bt*	Pl_r	Opx_r	Hbl_r	*Bt*	Pl_r	Opx_r	Hbl_r	*Bt*	Pl_r
SiO_2	49.88	34.23	50.21	56.20	46.83	37.50	56.46	52.79	47.84	37.91	56.36	53.06	47.52	38.12	56.99
TiO_2	0.00	4.94	0.00	0.00	0.94	3.58	0.00	0.03	0.59	2.13	0.00	0.00	0.75	2.43	0.00
Al_2O_3	0.61	14.94	31.51	27.87	10.46	15.69	27.34	1.25	8.65	17.07	27.59	1.14	10.27	15.54	27.18
FeO	33.07	20.83	0.44	0.34	12.85	13.80	0.27	21.41	14.27	9.61	0.29	22.27	12.99	12.15	0.58
MnO	0.80	0.06	0.00	0.00	0.62	0.23	0.00	5.90	2.42	0.36	0.00	3.23	1.21	0.52	0.00
MgO	14.20	9.03	0.00	0.00	14.29	15.70	0.00	19.23	14.30	16.60	0.00	20.70	13.82	16.17	0.00
CaO	0.84	0.06	13.74	9.37	10.69	0.08	9.14	0.58	8.04	0.06	9.12	0.58	10.33	0.11	9.37
Na_2O	0.00	0.00	3.37	6.03	1.10	0.00	6.76	0.00	0.67	0.10	6.06	0.00	1.29	0.01	6.22
K_2O	0.00	9.01	0.11	0.34	0.44	9.32	0.10	0.00	0.40	9.80	0.21	0.00	0.41	9.20	0.29
Total	99.40	93.51[4]	99.38	100.15	98.22	95.40	100.07	101.19	97.18	93.64	99.63	100.98	98.59	94.25	100.63
X_{Mg}	0.428	0.436	–	–	0.654	0.666	–	0.556	0.604	0.748	–	0.591	0.634	0.695	–
X_{An}	–	–	0.688	0.453	–	–	0.425	–	–	–	0.448	–	–	–	0.447
Wo	1.8	–	–	–	–	–	–	1.3	–	–	–	1.2	–	–	–
En	42.6	–	–	–	–	–	–	60.7	–	–	–	61.6	–	–	–
Fs	55.6	–	–	–	–	–	–	38.0	–	–	–	37.2	–	–	–
T, °C	700 (*Cpx–Opx*)														

Table 2. (Contd.)

Component	Sample 537-S								Sample 576						
	Cpx–Opx–Pl hornfels				*Bt–Hbl–Opx–Pl* migmatite veinlet				*Bt–Opx–Pl–Or* metasomatite				*Bt–Opx–Pl–Or* migmatite veinlet		
	Cpx_r	Opx_r	Hbl_r	Pl_r	Opx_r	Hbl_r	*Bt*	Pl_r	Opx_r	*Bt*	Pl^1	Pl^2	Opx_r	*Bt*	Pl_r
SiO_2	52.77	54.20	47.19	51.42	53.90	46.31	38.47	56.68	48.21	36.48	56.68	59.47	50.44	35.70	60.09
TiO_2	0.14	0.00	1.01	0.00	0.00	0.95	3.09	0.00	0.04	4.36	0.00	0.00	0.06	5.13	0.00
Al_2O_3	2.45	1.33	9.70	31.77	1.35	9.95	13.99	28.37	8.76	17.20	28.37	25.89	4.86	15.99	25.07
FeO	7.19	16.86	8.81	0.24	18.45	10.56	9.14	0.38	21.74	13.53	0.38	0.09	21.74	15.09	0.23
MnO	0.95	1.24	0.32	0.00	2.04	0.51	0.17	0.00	1.19	0.20	0.00	0.00	1.06	0.15	0.00
MgO	4.32	25.19	15.99	0.00	23.61	15.08	17.97	0.00	20.19	13.01	0.00	0.00	22.04	13.09	0.00
CaO	21.97	0.50	11.32	14.07	0.49	11.67	0.00	9.54	0.14	0.02	9.54	7.26	0.10	0.00	7.19
Na_2O	0.11	0.00	1.22	3.19	0.00	1.11	0.00	6.08	0.00	0.00	6.08	7.88	0.00	0.00	7.63
K_2O	0.00	0.00	1.01	0.18	0.00	1.26	10.58	0.33	0.00	10.40	0.33	0.22	0.00	10.39	0.42
Total	99.90	99.32	96.57	100.87	99.84	97.40	93.41	101.38	100.27	95.20	101.38	100.81	100.30	95.54	100.63
X_{Mg}	0.758	0.712	0.757	–	0.672	0.708	0.775	–	0.611	0.628	–	–	0.633	0.605	–
X_{An}	–	–	–	0.705	–	–	–	0.456	–	–	0.456	0.333	–	–	0.334
Wo	46.3	1.0	–	–	1.0	–	–	–	0.3	–	–	–	0.2	–	–
En	41.9	72.0	–	–	68.8	–	–	–	61.2	–	–	–	64.2	–	–
Fs	11.8	27.0	–	–	30.2	–	–	–	37.5	–	–	–	35.6	–	–
T, °C	799 (*Cpx–Opx*)														

Component	Sample 585-D					Sample 539-Zh					Sample 540-L				
	Bt–Opx–Pl metasomatite			*Bt–Opx–Pl* migmatite veinlet		*Opx–Pl* metasomatite		*Bt–Opx–Pl* migmatite veinlet			*Bt–Cpx–Opx–Pl* metasomatite				
	Opx_r	*Bt*	Pl_r	Opx_r	Pl_r	Opx_r	Pl_r	Opx_r	*Bt*	Pl_r	Opx_r	*Bt*	Pl^1	Pl^2	Cpx_r
SiO_2	52.33	37.47	55.36	5253	57.62	51.61	58.33	51.58	36.89	58.06	51.83	37.76	51.14	53.82	52.71
TiO_2	0.00	5.02	0.00	0.03	0.00	0.00	0.00	0.18	4.25	0.00	0.69	4.16	0.00	0.00	0.00
Al_2O_3	1.94	15.68	28.63	1.16	27.42	3.87	26.17	2.58	15.29	26.63	0.66	14.81	31.30	29.62	0.67
FeO	22.62	12.66	0.47	21.42	0.19	23.33	0.44	23.44	13.96	0.21	27.37	13.92	0.43	0.35	10.00
MnO	0.61	0.10	0.00	0.80	0.00	1.57	0.00	1.06	0.06	0.00	0.49	0.02	0.00	0.00	0.19
MgO	21.62	14.29	0.00	21.51	0.00	19.60	0.00	21.51	13.86	0.00	18.71	14.04	0.00	0.00	13.43
CaO	0.42	0.02	10.49	0.64	9.11	0.16	8.19	0.14	0.02	8.38	0.65	0.02	14.14	12.16	21.77
Na_2O	0.00	0.00	5.30	0.00	6.23	0.00	6.50	0.00	0.00	6.30	0.00	0.00	3.52	4.58	0.00
K_2O	0.00	10.62	0.40	0.00	0.63	0.00	0.55	0.00	10.28	0.61	0.00	9.61	0.10	0.12	0.00
Total	99.54	95.76	100.65	98.09	101.20	100.14	100.18	100.49	94.61	100.19	100.40	94.89[5]	100.63	100.65	98.77
X_{Mg}	0.624	0.666	–	0.663	–	0.584	–	0.610	0.638	–	0.548	0.642	–	–	0.701
X_{An}	–	–	0.510	–	0.431	–	0.398	–	–	0.409	–	–	0.686	0.591	–
Wo	0.9	–	–	1.3	–	0.4	–	0.3	–	–	1.3	–	–	–	45.1
En	62.5	–	–	63.3	–	59.7	–	61.9	–	–	54.2	–	–	–	38.7
Fs	36.6	–	–	35.4	–	39.6	–	37.8	–	–	44.5	–	–	–	16.2
T, °C															

Table 2. (Contd.)

Component	Sample 540-L				Sample 427-L										
	Bt–Opx–Pl migmatite veinlet				*Bt–Opx–Pl* metasomatite			*Crt–Bt–Pl* migmatite veinlet				*Bt–Opx–Pl* migmatite veinlet			
	Opx_c	Opx_r	*Bt*	Pl_r	Opx_r	*Bt*	Pl_r	Grt_c	Grt_r	*Bt*	Pl_r	Opx_r	*Bt*	*Hbl*	Pl_r
SiO_2	51.30	51.58	36.44	58.07	51.60	34.83	54.89	37.96	37.56	35.10	58.12	51.08	35.15	45.37	55.85
TiO_2	0.02	0.05	4.46	0.00	0.20	4.84	0.00	0.00	0.00	4.16	0.00	0.01	4.04	0.45	0.00
Al_2O_3	1.21	0.98	14.82	26.95	0.81	14.83	28.77	22.11	22.02	15.24	26.68	0.67	14.38	9.10	28.40
FeO	29.74	28.88	17.77	0.27	28.58	23.05	0.55	27.59	28.13	23.01	0.11	30.69	23.17	16.68	0.29
MnO	0.62	0.64	0.05	0.00	0.77	018	0.00	6.21	5.79	0.20	0.00	0.80	0.08	0.14	0.00
MgO	17.78	17.02	11.69	0.00	16.30	7.98	0.00	4.30	3.75	8.49	0.00	16.10	8.54	11.64	0.00
CaO	0.39	0.43	0.03	8.57	0.91	0.02	10.95	3.57	3.75	0.00	8.48	0.70	0.01	11.03	10.02
Na_2O	0.00	0.00	0.03	6.43	0.00	0.00	5.32	0.00	0.00	0.00	6.88	0.00	0.00	0.86	5.80
K_2O	0.00	0.00	10.00	0.28	0.00	9.06	0.22	0.00	0.00	9.61	0.21	0.00	9.17	0.82	0.03
Total	101.06	99.58	95.29	100.59	99.17	94.83	100.70	101.73	101.64	95.81	100.48	100.05	94.54	96.13	100.40
X_{Mg}	0.511	0.507	0.540	–	0.497	0.380	–	0.184	0.166	0.395	–	0.477	0.396	0.552	–
X_{An}	–	–	–	0.417	–	–	0.525	*Alm*-59.9	*Alm*-62.5	–	0.400	–	–	–	0.488
Wo	0.8	0.9	–	–	2.0	–	–	*Prp*-16.6	*Prp*-15.3	–	–	1.5	–	–	–
En	51.2	50.8	–	–	49.4	–	–	*Sps*-13.6	*Sps*-14.3	–	–	47.6	–	–	–
Fs	48.0	48.3	–	–	48.6	–	–	*Grs*-9.9	*Grs*-79	–	–	50.9	–	–	–
T, °C								734 (*Crt–Bt*)							

Note: the total additionally includes V_2O_3 (in wt %): 1 – 0.05, 2 – 0.35; 3 – 0.11, 4 – 0.36; 5 – 0.55.

Table 3. Representative microprobe analyses of minerals from garnet enderbites (samples 535-E, 535-Z, 535-B, 539-V), charnockitoids (sample 575-B), garnet–cordierite–biotite plagiogneisses (sample 528-I), and hornfel enclaves (samples 535-V, 535-Z-1, 535-E-1) in garnet enderbites

Component	Sample 535-E						Sample 533-Z						Sample 535-B		
	Grt_r	Opx_r	Crd_r	*Bt*	*Pl*	Spl_r	Grt_r	Opx_r	Crd_r	*Bt*	*Pl*	*Or*	Grt_r	Opx_r	Crd_r
SiO_2	38.34	50.46	49.04	34.92	60.90	0.00	38.07	50.51	48.50	36.65	61.79	63.36	38.16	49.22	48.29
TiO_2	0.00	0.03	0.00	2.30	0.00	0.34	0.00	0.05	0.00	3.11	0.00	0.00	0.00	0.06	0.00
Al_2O_3	22.00	4.47	33.47	18.31	25.18	59.40	22.18	4.65	33.45	18.27	24.30	19.07	22.64	5.04	33.64
FeO	29.28	27.86	7.04	17.08	0.09	16.87	30.09	27.70	7.01	16.21	0.12	0.02	29.95	28.22	6.90
MnO	1.06	0.44	0.08	0.10	0.00	0.16	1.44	0.52	0.11	0.06	0.00	0.00	1.18	0.47	0.10
MgO	8.14	17.49	8.75	12.23	0.00	5.64	8.04	16.91	8.40	11.51	0.00	0.00	7.26	16.42	8.49
CaO	1.07	0.14	0.01	0.01	5.89	0.00	0.98	0.14	0.01	0.00	5.96	0.27	1.06	0.10	0.01
Na_2O	0.00	0.00	0.00	0.00	7.80	0.00	0.00	0.00	0.00	0.00	8.32	1.26	0.00	0.00	0.00
K_2O	0.00	0.00	0.00	9.03	0.53	0.00	0.00	0.00	0.00	10.18	0.23	15.46	0.00	0.00	0.00
Total	99.89	100.89	99.38	93.98	100.39	101.41[1]	100.80	100.56[2]	97.48	95.99	100.72	99.44	100.25	99.53	97.43
X_{Mg}	0.323	0.524	0.687	0.559	–	0.371	0.312	0.516	0.678	0.558	–	–	0.294	0.505	0.684
X_{An}	–	–	–	–	0.285	–	–	–	–	–	0.280	–	–	–	–
Wo	–	0.3	–	–	–	–	–	0.3	–	–	–	–	–	0.2	–
En	–	52.6	–	–	–	–	–	51.9	–	–	–	–	–	50.8	–
Fs	–	47.1	–	–	–	–	–	47.8	–	–	–	–	–	49.0	–
Alm	63.3	–	–	–	–	–	63.8	–	–	–	–	–	65.9	–	–
Prp	31.4	–	–	–	–	–	30.4	–	–	–	–	–	28.5	–	–
Sps	2.3	–	–	–	–	–	3.1	–	–	–	–	–	2.6	–	–
Grs	3.0	–	–	–	–	–	2.7	–	–	–	–	–	3.0	–	–
T, °C	754–776 (*Grt–Bt*)						759–804 (*Grt–Bt*)						690–697 (*Grt–Bt*)		
P_s, kbar	4.2–4.4(*Grt–Opx–Pl*)						3.7–4.0 (*Grt–Opx–Pl*)						3.4 (*Grt–Opx–Pl*), 4.8 (*Grt–Opx*)		

Table 3. (Contd.)

Component	Sample 535-B		Sample 539-B					Sample 575-B						Sample 528-I	
	Bt	Pl_r	Crt_r	Opx_r	*Bt*	Pl_r	*Or*	*Cpx*	Opx_r	*Bt*	Pl^1	Pl^2	*Spl*	Grt_r	*Bt*
SiO_2	35.68	60.00	38.80	49.31	36.39	60.76	64.78	51.96	53.04	37.66	56.42	61.06	0.00	37.96	36.36
TiO_2	5.16	0.00	0.00	0.11	5.20	0.00	0.00	0.43	0.00	4.07	0.00	0.00	0.58	0.00	3.50
Al_2O_3	17.71	25.08	22.58	5.03	17.29	24.80	18.51	2.95	0.99	15.17	27.60	24.43	63.60	22.15	17.78
FeO	15.71	0.02	29.89	28.13	17.28	0.15	0.00	8.68	21.30	15.12	0.23	0.20	20.88	30.71	15.73
MnO	0.08	0.00	1.14	0.40	0.01	0.00	0.00	0.30	0.63	0.17	0.00	0.00	0.27	1.49	0.07
MgO	12.66	0.00	7.64	16.88	10.60	0.00	0.00	13.10	22.99	12.95	0.00	0.00	11.40	6.52	11.53
CaO	0.02	6.46	1.08	0.11	0.02	6.30	0.02	20.98	0.56	0.06	9.38	6.10	0.00	1.40	0.01
Na_2O	0.00	8.02	0.00	0.00	0.00	7.57	0.01	0.19	0.00	0.00	5.84	7.82	0.00	0.00	0.04
K_2O	9.53	0.28	0.00	0.00	10.06	0.43	16.85	0.01	0.00	10.67	0.44	0.43	0.00	0.00	9.93
Total	96.55	99.89	101.13	99.97	96.85	100.01	100.17	98.60	99.51	95.87	99.91	100.04	102.16[3]	100.23	94.95
X_{Mg}	0.588	–	0.305	0.513	0.0522	–	–	0.722	0.651	0.601	–	–	0.490	0.265	0.565
X_{An}	–	0.304	–	–	–	0.307	–	–	–	–	0.458	0.294	–	–	–
Wo	–	–	–	0.2	–	–	–	45.7	1.2	–	–	–	–	–	–
En	–	–	–	51.6	–	–	–	39.6	65.0	–	–	–	–	–	–
Fs	–	–	–	48.2	–	–	–	14.7	33.8	–	–	–	–	–	–
Alm	–	–	64.9	–	–	–	–	–	–	–	–	–	–	67.3	–
Prp	–	–	29.6	–	–	–	–	–	–	–	–	–	–	25.5	–
Sps	–	–	2.5	–	–	–	–	–	–	–	–	–	–	3.3	–
Grs	–	–	3.0	–	–	–	–	–	–	–	–	–	–	3.9	–
T, °C	690–697 (*Grt–Bt*)		771–796 (*Grt–Bt*)					744 (*Opx–Cpx*)						678 (*Grt–Bt*)	
P_s, kbar	3.2–3.4(*Grt–Opx–Pl*), 4.85 (*Grt–Opx*)		3.6–3.9 (*Grt–Opx–Pl*)												

Table 3. (Contd.)

Component	Sample 528-I	Sample 535-V					Sample 535-Z-1					Sample 535-E-1				
	Pl$_r$	*Crt*^{1}	*Crt*^{2}	*Opx*	*Bt*	*Pl*$_r$	*Opx*^{1}	*Opx*^{2}	*Grd*	*Pl*^{1}	*Pl*^{2}	*Cpx*$_r$	*Pl*^{1}	*Opx*$_r$	*Bt*$_r$	*Pl*^{2}
SiO_2	59.95	3809	37.57	50.45	34.63	57.34	53.96	50.58	49.17	56.02	60.17	53.21	46.29	52.84	37.22	49.51
TiO_2	0.00	0.00	0.05	0.13	3.84	0.00	0.00	0.08	0.00	0.00	0.00	0.12	0.00	0.04	4.20	0.00
Al_2O_3	25.07	22.50	22.03	4.63	17.83	27.14	2.21	4.79	33.69	28.61	24.94	1.24	34.51	2.10	16.42	32.55
FeO	0.06	30.88	29.01	26.56	18.42	0.42	20.03	28.13	6.87	0.26	0.06	6.48	0.14	21.84	11.46	0.45
MnO	0.00	1.94	1.46	0.46	0.11	0.00	0.42	0.52	0.09	0.00	0.00	0.19	0.00	0.41	0.00	0.00
MgO	0.00	5.37	7.74	17.45	9.46	0.00	23.63	16.74	8.64	0.00	0.00	14.59	0.00	22.18	14.85	0.00
CaO	7.14	1.85	1.50	0.14	0.04	9.13	0.16	0.09	0.00	10.59	5.93	22.36	17.18	0.21	0.06	15.26
Na_2O	7.55	0.00	0.00	0.00	0.00	6.48	0.00	0.00	0.00	5.00	8.23	0.02	1.59	0.00	0.24	2.89
K_2O	0.09	0.00	0.00	0.00	9.03	0.40	0.00	0.00	0.00	0.28	0.41	0.00	0.03	0.00	9.83	0.05
Total	99.86	100.63	99.36	98.82	93.36	100.91	100.49^4	100.93	98.46	100.76	99.74	98.39^5	99.74	99.62	94.75^6	100.71
X_{Mg}	–	0.226	0.311	0.535	0.476	–	0.673	0.510	0.689	–	–	0.796	–	0.640	0.698	–
X_{An}	0.341	–	–	–	–	0.428	–	–	–	0.530	0.278	–	0.855	–	–	0.742
Wo	–	–	–	0.3	–	–	0.3	0.2	–	–	–	46.9	–	0.4	–	–
En	–	–	–	53.8	–	–	67.5	51.4	–	–	–	42.5	–	64.1	–	–
Fs	–	–	–	45.9	–	–	32.2	48.4	–	–	–	10.6	–	35.5	–	–
Alm	–	68.9	62.7	–	–	–	–	–	–	–	–	–	–	–	–	–
Prp	–	21.4	29.9	–	–	–	–	–	–	–	–	–	–	–	–	–
Sps	–	4.4	3.2	–	–	–	–	–	–	–	–	–	–	–	–	–
Grs	–	5.3	4.2	–	–	–	–	–	–	–	–	–	–	–	–	–
T, °C		779 (*Crt–Opx*)														
P_s, kbar		3.5–3.7 (*Crt–Opx–Pl*)														

Note: the total additionally includes the following (wt%): 1 – 14.6 ZnO, 3.29 Cr_2O_3, 0.22 V_2O_3; 2 – 0.08 Cr_2O_3; 3 – 0.60 Cr_2O_3, 4.83 ZnO; 4 – 0.08 Cr_2O_3; 5 – 0.18 Cr_2O_3; 6 – 0.47 Cr_2O_3. The temperature and pressure were calculated from internally consistent geothermobarometers [1].

Table 4. Chemical composition of basic hornfelses, metasedimentary rocks of the Vakhtalkinskaya sequence, and products of their metasomatic alteration and magmatic replacement in the contact aureole of the Yurchik intrusion

Component	Clinopyroxene–amphibole–plagioclase±orthopyroxene hornfelses									Amphibole–plagioclase hornfelses			
	427-V	528-V	531-B	537-N	538-B	538-G	538-O	539	539-Zh	426-A	426-B	428-B	537-L
	1	2	3	4	5	6	7	8	9	10	11	12	13
SiO_2	51.95	49.65	48.85	49.38	51.58	51.42	53.75	53.05	48.20	47.40	48.41	47.20	45.50
TiO_2	0.69	0.83	0.79	1.44	1.38	1.54	1.00	0.90	1.37	1.24	1.50	1.36	1.18
Al_2O_3	17.53	14.09	9.45	15.77	17.65	17.69	17.95	16.87	15.96	16.44	16.63	16.70	17.37
Fe_2O_3	2.05	4.92	3.62	2.72	2.20	2.71	4.82	4.74	3.58	3.75	10.28*	3.98	11.21*
FeO	4.78	5.96	8.33	5.68	4.64	4.94	3.84	4.18	4.51	5.86		4.54	
MnO	0.19	0.21	0.22	0.17	0.09	0.19	0.17	0.23	0.16	0.15	0.20	0.12	0.17
MgO	8.50	10.62	12.43	8.37	5.70	4.70	5.04	5.05	4.56	8.77	8.44	10.42	9.53
CaO	11.26	7.09	12.27	12.64	12.56	13.01	8.83	11.30	15.02	10.51	10.75	8.78	11.45
Na_2O	1.75	2.63	1.13	2.43	3.24	3.10	3.44	2.86	2.43	3.52	2.99	4.19	2.27
K_2O	0.51	1.16	0.74	0.88	0.77	0.37	1.01	0.74	0.97	0.47	0.47	0.83	0.44
P_2O_5	n.d.	n.d.	n.d.	n.d.	n.d.	n.d.	n.d.	n.d.	n.d.	0.05	0.12	0.24	0.15
L.O.I.	0.80	2.46	2.14	0.58	0.27	0.25	0.38	0.19	3.15	1.28	0.49	1.20	0.65
Total	100.01	99.62	99.97	100.06	100.08	99.92	100.23	100.11	99.91	99.44	100.29	99.56	99.92

Component	Amphibole–plagioclase hornfels		Biotite–orthopyroxene–plagioclase metasomatites										
	591-B	532	427-D	427-I	427-L	427-N	537-O	537-R	537-Kh	538-K	538-M	538-S	539-T
	14	15	16	17	18	19	20	21	22	23	24	25	26
SiO_2	53.25	53.45	54.18	56.55	51.17	50.71	53.29	53.20	55.47	54.45	56.10	53.56	53.03
TiO_2	0.70	0.79	0.73	0.87	0.85	0.78	0.85	0.76	0.73	0.70	0.86	0.77	0.91
Al_2O_3	18.63	16.64	19.76	18.99	21.99	21.64	21.94	21.37	18.32	21.99	20.92	21.60	21.56
Fe_2O_3	3.15	5.87	6.27	1.31	9.11*	8.14*	4.96	3.89	5.02	3.80	3.01	5.07	4.09
FeO	3.60	4.32	1.67	6.37			2.44	2.71	2.14	2.84	3.11	2.84	3.51
MnO	0.16	0.17	0.16	0.18	0.14	0.30	0.15	0.09	0.15	0.11	0.15	0.14	0.13
MgO	5.88	5.76	3.50	3.69	3.52	3.92	2.86	2.76	3.33	3.10	3.03	2.95	1.95
CaO	7.74	7.01	8.78	7.41	7.68	8.82	8.52	10.04	8.35	8.18	7.39	8.69	8.71
Na_2O	4.64	4.54	3.91	3.22	3.70	4.39	3.96	3.84	3.91	3.96	4.45	3.80	4.25
K_2O	0.53	0.21	0.84	0.42	1.23	0.56	0.82	1.23	1.28	0.87	0.51	0.62	1.37
P_2O_5	n.d.	n.d.	n.d.	n.d.	0.21	0.49	n.d.	n.d.	n.d.	n.d.	n.d.	n.d.	n.d.
L.O.I.	1.50	1.30	0.17	0.50	0.55	0.24	0.13	0.13	1.20	0.03	0.31	0.02	0.42
Total	99.78	100.06	99.97	99.51	100.15	99.99	99.92	100.02	99.90	100.03	99.84	100.06	99.93

Table 4. (Contd.)

Component	Biotite–orthopyroxene–plagioclase metasomatites				Garnet enderbites and garnet–cordierite–biotite plagiogneisses							
	574-B	574-B-1	574-L	535-K	539-B	539-A	536-V	420-E	420-Z	428	428-Zh	434-A
	27	28	29	30	31	32	33	34	35	36	37	38
SiO_2	54.80	59.89	52.90	59.01	66.28	61.83	68.38	63.02	62.62	62.30	59.82	56.14
TiO_2	0.73	0.86	0.85	0.76	0.78	0.86	0.81	0.93	0.69	1.04	1.09	0.99
Al_2O_3	17.70	15.22	19.66	18.17	15.44	18.26	13.70	16.96	15.38	15.90	18.35	17.50
Fe_2O_3	9.21*	8.34*	1.44	6.87*	6.84*	5.45*	6.50*	2.34	2.08	2.75	0.47	1.70
FeO			6.47					5.10	4.85	4.54	6.24	5.86
MnO	0.19	0.14	0.35	0.11	0.10	0.07	0.08	0.08	0.17	0.12	0.08	0.08
MgO	3.52	3.16	5.29	3.46	2.72	5.48	2.54	2.89	3.29	2.99	2.99	4.54
CaO	6.10	4.22	6.86	5.60	2.39	2.67	2.07	2.02	2.99	2.88	3.46	3.31
Na_2O	3.78	3.10	2.92	4.12	3.06	2.53	2.69	2.97	3.81	2.97	3.65	4.19
K_2O	0.76	1.47	0.95	1.69	1.15	1.33	1.22	1.34	2.18	1.07	1.24	1.07
P_2O_5	0.19	0.25	n.d.	0.15	0.08	0.18	0.08	0.11	n.d.	0.16	0.31	0.16
L.O.I.	1.31	0.99	1.71	0.68	1.82	1.54	1.89	2.04	1.29	2.76	2.41	3.82
Total	98.29	97.64	99.40	100.62	100.66	100.20	96.96	99.80	99.35	99.48	100.11	99.36

Component	Garnet enderbites and plagiogneisses		Charnockitoids			Metadacites				Xenolith hornfelses from garnet enderbites		
	535-L	537-U	373-A	575	575-B	591	591-A	433-A	434	535-V	535-L	557-L
	39	40	41	42	43	44	45	46	47	48	49	50
SiO_2	56.17	63.32	64.34	31.95	35.88	66.55	67.35	64.84	70.17	65.20	56.91	51.15
TiO_2	1.05	1.10	0.91	1.09	0.90	0.43	0.37	0.24	0.39	064	0.53	0.66
Al_2O_3	18.59	16.82	15.99	16.84	15.91	16.18	16.64	18.03	13.91	15.85	12.27	11.86
Fe_2O_3	3.62	2.52	2.85	2.93	5.58*	3.39	1.53	2.52	1.71	0.55	11.28*	1.23
FeO	8.02	4.51	2.25	3.50		2.67	2.26	1.51	2.88	6.37		9.02
MnO	0.17	0.13	0.05	0.20	0.08	0.13	0.10	0.20	0.13	0.19	0.22	0.18
MgO	4.53	3.53	2.43	2.66	1.58	1.11	0.49	1.34	2.09	5.06	11.46	16.73
CaO	3.05	2.74	1.01	5.30	3.46	5.22	5.06	2.88	1.29	1.60	7.01	7.22
Na_2O	3.24	3.24	5.04	2.92	3.88	3.56	4.21	5.48	4.58	2.92	0.72	2.81
K_2O	0.78	0.86	4.2	1.49	2.31	0.64	0.85	1.21	1.95	0.62	0.36	0.40
P_2O_5	n.d.	n.d.	0.13	n.d.	0.18	n.d.	n.d.	0.26	0.12	n.d.	0.04	n.d.
L.O.I.	0.86	1.30	0.42	0.60	0.30	0.56	0.76	1.21	0.26	0.40	0.00	0.69
Total	100.08	100.07	99.68	99.48	100.06	100.44	99.62	99.62	99.48	99.40	100.80	101.95

Notes: * – All the iron is as Fe_2O_3. Sample 574-B-1 is the biotite–orthopyroxene–plagioclase migmatite veinlet in biotite–orthopyroxene–plagioclase metasomatites. n.a. – not analyzed.

Table 5. Geochemical characteristics of basic hornfelses, metasedimentary rocks of the Vakhtalkinskaya Sequence, and products of their metasomatic and magmatic replacement

Element	Amphibole–plagioclase hornfels			Biotite–orthopyroxene–plagioclase metasomatites					Garnet enderbites and plagiogneisses			Charnockitoids	Xenoliths hornfelses from garnet enderbites	
	425-V	426-B	537-L	427-L	427-N	535-K	574-B	574-B-1	539-B	539-A	536-V	575-B	535-L	557-L
Rb	23	3	3	37	4	26	16	42	18	22	32	27	22	22
Sr	567	193	706	760	1862	477	613	429	317	640	265	297	108	143
Ba	428	55	167	1589	552	560	522	1076	664	1175	535	1524	240	359
Y	19	26	39	20	21	21	20	18	24	15	13	30	13	13
Zr	80	75	57	130	145	110	96	203	209	335	241	402	36	38
Nb	6	3	4	6	4	6	5	7	7	6	9	8	3	2
Pb	4	2	2	11	7	12	9	9	11	10	11	10	4	4
Th				3		5	4	3	3	5	4	2	1	1
V	255	242	351	247	228	226	236	216	157	141	152	105	240	223
Cr	81	226	259	46	32	71	47	101	104	19	108	18	817	828
Co	24	36	31	22	22	18	20	21	13	6	12	7	46	57
Ni	28	134	39	24	45	27	19	35	26	5	27	7	199	273
Cu	122	38	367	85	10	30	39	122	132	14	47	19	11	7
Zn	79	73	104	69	98	42	93	82	122	76	65	72	113	88
Ga	19	16	21	22	25	20	19	17	16	18	14	16	15	12
S	0.240	0.011	0.075	0.192	0.003	0.003	0.081	0.292	0.274	0.007	0.279	0.005	0.049	0.003
Cl	0.00	0.003	0.010	0.018	0.024	0.026	0.015	0.013	0.003	0.004	0.005	0.009	0.004	0.005

Note: The contents of S and Cl are given in wt %, and other elements, in ppm. The analyses were performed using XRF on an automated S_4 Pioneer spectrometer at the Analytical Center of the Far East Geological Institute of the Far East Branch of the Russian Academy of Sciences.

inner parts of the contact aureole of the Yurchik gabbronorite intrusion. The steep almost vertical dip of the intrusive contacts determined the small thickness of the high-temperature contact hornfelses (up to a few tens of meters). The wide area of high-temperature metamorphic transformations (formation of hornfelses, metasomatism, and magmatic replacement) of primary terrigenous–volcanogenic rocks was noted only in the northern part of the massif, where geophysical studies defined the largest thickness of the intrusive body, magma conduits, and gabbronorite apophyses among the thin cap of the host rocks of the Vakhtalkinskaya sequence (Fig 1).

Several stages of transformations can be arbitrarily distinguished based on the study of the mineral assemblages of the altered rocks of the Vakhtalkinskaya sequence in the contact aureole. All these stages occurred simultaneously, have tight spatiotemporal relations, and were determined by the intensity of the effect of mantle fluids, which filtered through magmatic channels serving as pathways for gabbroid melt.

The first stage is the stage of contact metamorphism related to the emplacement of the gabbroid intrusion. This stage was responsible for transformation of the initial basic volcanics into amphibole, clinopyroxene–amphibole, and two pyroxene-amphibole hornfelses, while sedimentary interlayers were converted into garnet–biotite and garnet–cordierite–biotite hornfelses. The temperature of the contact metamorphism is estimated at 700–800°C.

The second stage led to the metasomatic alteration of aureole hornfelses and formation of bodies of biotite–orthopyroxene–plagioclase metasomatites. Metasomatically altered rocks rarely form large outcrops; more often they occur as irregularly shaped bodies of limited sizes (occasionally as small as tens of centimeters) among the basic metavolcanics of the Vakhtalkinskaya sequence. Large exposures of metasomatites were found in the boudinaged metasedimentary intercalations (Fig. 3).

During the third stage, the metasomatically altered basic hornfelses were subjected to partial melting to form migmatite veinlets and patches of biotite–orthopyroxene–plagioclase±garnet composition. During magmatic replacement, interbeds of sedimentary hornfelses were transformed into bodies of garnet enderbites and plagiogneisses. The use of modern internally consistent mineral geobarometers [1] showed that these granulite-like rocks were formed at a temperature of 700–800°C and moderate depths (12–17 km) corresponding to lithostatic pressure of 3.2–.4.8 kbar (Table 3).

The comparison of the chemical composition of the initial basic volcanics of the Vakhtalkinskaya sequence from the contact aureole and products of their transformation (Tables 4, 5; Fig. 13) indicates that metasomatism and magmatic replacement correspond to siliceous–alkaline metasomatism (granitization), which was accompanied by a subsequent uneven influx of Si, Al, Na, K, Rb, Ba, Zr, Nb, and Cl and removal of Fe, Mg, Mn, Ca, and such trace components as Cr, Co, Ti, Y, and Sc, causing intense debasification of the initial rocks.

Granitization and magmatic replacement with formation of granitoids are widely spread processes representing sharply expressed debasification of the crustal substrate with removal of significant amounts of Ca, Mg, Fe, and often Al from the substrate and an influx of Si and alkalis [10, 14, 21, 22, 25, 26, 29, 48]. Granitization has been described in numerous works; the physicochemical principles of this process are considered in detail by D.S. Korzhinsky [21–24] and confirmed by numerous experimental studies [10–17, 29, 42].

The theoretical concepts determine the granitization as magmatic replacement of the initial rocks under the influence of ascending subcrustal transmagmatic fluids derived by mantle degassing [21, 22]. The magmatic replacement suggests that the granite formation and final melting of the metamorphic rocks postdate their metasomatic treatment by alkaline–siliceous fluids with debasification and bleaching, which occurred concurrently with increasing partial melting (formation of banded and shadow migmatites).

The granitizing fluids ascended through deep-seated fault zones that penetrated the mantle, zones of blastomylonites or strongly gneissose rocks [27], and melting zones in the mantle [14], because the melts accumulated volatiles extracting alkaline-siliceous components.

The analysis of the modern state of the granite formation problems [14] indicates that the main mechanisms of the formation of granitoid melts are the following: (1) granitization, i.e., allochemical melting with preliminary metasomatic treatment and subsequent replacement of the crustal rocks by the melt; and (2) thermal and chemical interaction between mantle magmas and crustal material, which generates hybrid granitoid melts [14, 43]. Extensive development of granites under deep-seated conditions leads to obliteration of their relations with the intrusion of the mantle melts that were responsible for their formation [30].

Granitization as magmatic replacement was provoked by deep-seated mantle-derived fluids [4, 9, 10, 14–16, 21, 22, 29, 42, 47, 48]. Experimental studies of the solubility of mantle material at high temperatures and pressures indicate that mantle fluids are highly concentrated aqueous solutions (up to 100 and more g/l [10, 15, 16]), which incongruently dissolve significant amounts of silica and alkalis, as well as some lithophile elements such as Li, Rb, and REE, in mantle rocks [10, 16, 47, 48].

A decrease in the pressure and temperature leads to the decrease of the solubility of silica and alkalis in mantle fluids and, as a result, to metasomatic alteration and allochemical partial melting of aluminosilicate crustal rocks, causing their granitization [16]. According to [15], the necessary conditions for these processes are: (1) high thermal heating of the zone of fluid influence (the temperature in the fluid discharge zone must be no less than the temperature of the granite solidus) and (2) a sufficiently thick crustal substrate (about 15–20 km) providing high solubility of the mantle material by fluids.

The presented factual material illustrates that the high thermal heating of the crustal substrate and its significant thickness are typical of the Ganal Ridge of Kamchatka, which determined the intense development of contact metamorphism, metasomatism, granitization, and magmatic replacement of primary basic volcanics and intercalated terrigenous rocks in the contact aureole of the Yurchik gabbronorite intrusion under the effect of mantle fluids that presumably were supplied through magmatic channels, which served as the pathways for gabbroid magma.

CONCLUSIONS

Based on the geological, mineralogical, and geothermobarometric data, the metamorphic alterations of primary terrigenous–volcanogenic rocks of the Vakhtalkinskaya sequence of the Ganal Group in Kamchatka and, correspondingly, the formation of high-temperature granulite-like rocks were caused by the contact-reaction effect of the large Yurchik gabbronorite intrusion.

The contact influence of the gabbroids whose temperature reached 700–800°C in the inner aureoles, caused the transformation of basic volcanics of the Vakhtalkinskaya sequence into two-pyroxene–plagioclase, clinopyroxene–amphibole–plagioclase, and amphibole–plagioclase hornfelses, while terrigenous intercalations were converted into garnet–biotite and garnet–cordierite–biotite hornfelses. Basic hornfelses were locally subjected to metasomatic alterations with formation of bodies of fine-grained biotite–orthopyroxene–plagioclase metasomatites. In the zones of most intense influence of mantle fluids, metasomatites suffered partial melting and magmatic replacement with formation of biotite–orthopyroxene–plagioclase±garnet magmatic veinlets and patches, while metaterrigenous interlayers were replaced by garnet enderbites and plagiogneisses formed at 700–800°C and 3.2–4.8 kbar, which corresponds to a depth of 12–17 km. The metasomatic transformation and magmatic replacement caused intense debasification of primary rocks, which was expressed in the increase of the plagioclase content in parallel to the decrease in the An component and increase of the Fe mole fraction in mafic minerals.

The comparison of the chemical composition of the mafic volcanics of the Vakhtalkinskaya sequence with products of their transformation showed that, chemically, the metasomatic alteration and magmatic replacement of the primary rocks correspond to siliceous–alkaline metasomatism (granitization) and cause a subsequent and uneven influx of Si, Al, Na, K, Rb, Ba, Zr, Nb, and Cl and removal of Fe, Mg, Mn, Ca, and some trace elements (Cr, Co, Ti, Y, and S).

It is suggested that the metamorphic processes involving a change of the primary rocks, their mineral assemblages, and the mineral composition of the Vakhtalkinskaya sequence of the Ganal Group were caused by highly mineralized mantle fluids, which ascended along magmatic channels, the pathways for gabbroid melt.

ACKNOWLEDGMENTS

We are grateful to the reviewers B.A. Markovsky and E.N. Gramenitsky, as well as to Corresponding Member of the Russian Academy of Sciences S.P. Korikovsky, for valuable comments and recommendations that were taken into account during the final editing of the manuscript.

REFERENCES

1. O. V. Avchenko, *Mineral Equilibrium in Metamorphic Rocks and Geobarothermometry* (Nauka, Moscow, 1990) [in Russian].
2. S. E. Aprelkov, B. V. Ivanov, and S. V. Popruzhenko, "Tectonics and Geodynamic Evolution of Southeastern Kamchatka (Petropavlovsk Geodynamic Ground)," Tikhookean. Geol. **18** (4), 16–28 (1999). 1
3. V. I. Vinogradov, M. I. Bujakaite, G. A. Goroshchenko, et al., "Isotopic and Geochronologic Features of High-Grade Rocks of the Ganal Ridge of Kamchatka," Dokl. Akad. Nauk SSSR **318** (4), 930–936 (1991).
4. S. N. Gavrikova and V. A. Zharikov, "Geochemistry of Granitization of the Archean Granulite Rocks in the Eastern Baikal Area," Geokhimiya **22** (1), 26–49 (1984).
5. *Geology of the USSR. Kamchatka, the Kuril and the Commander Islands. Geological Description* (Nedra, Moscow, 1964), Vol. 31 [in Russian].
6. L. L. German, "Structural Setting of Granulate," Sov. Geol. No. 7, 118–126 (1975). 1
7. L. L. German, V. I. Shul'diner, and S. A. Shcheka, "Metamorphic Complexes of the Ganal Ridge in Kamchatka," Izv. Akad. Nauk SSSR, Ser. Geol., No. 2, 25–35 1 (1976).
8. L. L. German, *Ancient Crystalline Rocks of Kamchatka* (Nedra, Moscow, 1978) [in Russian].
9. N. S. Gorbachev and G. A. Kashirtseva, "Fluid-Melt Interaction and Evolution of Oceanic Basalts," in *Sketches in Physicochemical Petrology*, Ed. by V. A. Zharikov and V. V. Fed'kin (Nauka, Moscow, 1985), No. 13, pp. 106–111 [in Russian].
10. N. S. Gorbachev and G. A. Kashirtseva, "Melt–Fluid Equilibrium: Experimental Model of Magmatic Fluid," in *Proceedings of Annual Session of Mineralogical Society Russian Mineralogical Society Dedicated to the 110th Anniversary of Academician A. G. Betekhtin on Role of Mineralogy in Knowledge of Ore-Forming Processes, Moscow, Russia, 2007* (Inst. Geochim. Miner.

Ross. Akad. Nauk, Moscow, 2007), pp. 116–118 [in Russian].

11. E. N. Gramenitsky, "Mechanism of Magmatic Replacement With Reference to Contact Zone of the Syrostanskii Massif at the Southern Urals," Vestn. Mosk. Univ.,
1 Ser. Geol., No. 3, 62–77 (1990).

12. E. N. Gramenitsky and P. V. Lukin, "Approach to Experimental Modeling of Magmatic Replacement," Vestn.
1 Mosk. Univ., Ser. Geol., No. 4, 16–26 (1996).

13. E. N. Gramenitsky, A. M. Batanova, and T. I. Shchekina, "Mechanisms of Processes of Assimilation and Magmatic Replacement," Izv. Sekt. Nauk Zemli Ross. Akad. Estestv. Nauk, No. 8, 50–63 (2002).

14. V. A. Zharikov, "Problems of Granite Formation," Vestn.
1 Mosk. Univ., Ser. Geol., No. 6, 3–14 (1987).

15. V. A. Zharikov, M. B. Epel'baum, and M. V. Bogolepov, "Experimental Study of Possible Granitization under the Effect of Deep-Seated Fluid," Dokl. Akad. Nauk SSSR **311** (2), 462–465 (1990).

16. V. A. Zharikov, M. B. Epel'baum, M. V. Bogolepov, and A. G. Simakin, "Processes of Granitization (Experimental Study, Numerical Model)," in *Experimental Problems of Geology*, Ed. by V. A. Zharikov and V. V. Fed'kin (Nauka, Moscow, 1994), pp. 83–104 [in Russian].

17. V. A. Zharikov, "Some Aspects of Granitization Prob-
1 lem," Vestn. Mosk. Univ., Ser. Geol., No. 4, 3–12 (1996).

18. V. P. Zinkevich, E. A. Konstantinovskaya, N. V. Tsukanov, et al., *Accretionary Tectonics of Eastern Kamchatka* (Nauka, Moscow, 1993) [in Russian].

19. V. P. Zinkevich, A. V. Rikhter, and M. M. Fuzgan, "^{40}Ar/^{39}Ar Dating of Metamorphic Rocks of Eastern Kamchatka," Dokl. Akad. Nauk **333** (4), 477–480 (1993).

20. *Map of the Mineral Resources of Kamchatka Area. 1:500000,* Ed. by A. F. Litvinov, M. G. Patoki, B. A. Mar-
1 kovsky, et al. (Vseross. Geol. Inst., St. Petersburg, 1999) [in Russian].

21. D. S. Korzhinsky, "Granitization as Magmatic Replace-
1 ment," Izv. Akad. Nauk SSSR, Ser. Geol., No. 2, 56–69 (1952).

22. D. S. Korzhinsky, "The Sketch of Metasomatic Processes," in *Main Problems in the Theory of Magmatogenic Ore Deposits,* Ed. by A. G. Betekhtin (Akad. Nauk SSSR, Moscow, 1955), pp. 335–453 [in Russian].

23. D. S. Korzhinsky, "Flows of Transmagmatic Solutions and Granitization," in *Magmatism, Formation of Crystalline Rocks and Earth's Interior*, Ed. by G. D. Afanas'ev (Nauka, Moscow, 1972), Part 1, pp. 144–153 [in Russian].

24. D. S. Korzhinsky, "Interaction between Magmas and Transmagmatic Fluids," Zap. Vseross. Mineral. O-va, No. 2, 173–178 (1977).

25. V. K. Kuz'min, V. A. Glebovitsky, B. V. Belyatsky, et al., "Cenozoic Granulites of the Ganal Ridge, Eastern Kamchatka," Dokl. Akad. Nauk **393** (3), 371–375 (2003) [Dokl. Earth Sci. **393A** (9), 1211–1220 (2003)].

26. F. A. Letnikov, *Granitoids of Block-Fault Areas* (Nauka, Novosibirsk, 1975) [in Russian].

27. F. A. Letnikov, S. O. Balyshev, and V. V. Lashkevich, "Interrelations among the Processes of Granitization, Metamorphism, and Tectonics," Geotektonika **34** (1), 3–22 (2000) [Geotectonics **34** (1), 1–18 (2000)].

28. M. V. Luchitskaya and A. V. Rikhter, "Geotectonic Delamination of Metamorphic Rocks of the Ganal Ridge (Kamchatka)," Geotektonika **24** (2), 76–85 (1989).

29. A. A. Marakushev, *Magmatic Replacement and Its Petrogenetic Role*, in *Sketches in Petrogenetic Petrology*, Ed. by V. A. Zharikov (Nauka, Moscow, 1987), No. 14, pp. 24–38 [in Russian].

30. A. A. Marakushev, *Petrogenesis* (Nedra, Moscow, 1988) [in Russian].

31. A. V. Rikhter, "On Structure of Metamorphic Complexes of the Ganal Ridge (Kamchatka)," Geotektonika **26** (1), 98–108 (1991).

32. O. M. Rozen and M. S. Markov, "Genesis of Amphibolites of Metamorphic Melanocratic Basement of Island Arcs: Evidence from the Ganal Ridge, Kamchatka," Geotektonika **8** (3), 27–39 (1973).

33. I. A. Tararin, "Genesis of Granulites of the Ganal Ridge, Kamchatka," Dokl. Akad. Nauk SSSR **234** (3), 677–680 (1977).

34. I. A. Tararin, "Evolution of Metamorphic Processes in the Ganal Ridge, Kamchatka," in *Correlation of Endogenic Processes of the Pacific Belt*, Ed. by S. S. Zimin (Dal'nevost. Otd. Ross. Akad. Nauk, Vladivostok, 1979), pp. 63–101 [in Russian].

35. I. A. Tararin, "Magmatic Replacement at the Contact of Gabbroids and Plagiogneises in the Ganal Ridge, Kamchatka," Dokl. Akad. Nauk SSSR **247** (1), 179–184 (1979).

36. I. A. Tararin, "Genesis of Charnockite-like Rocks in the Metamorphic Complex of the Ganal Ridge, Kamchatka," Izv. Akad. Nauk SSSR, Ser. Geol., No. 6, 45–57 1
(1982).

36. I. A. Tararin, V. M. Chubarov, and T. M. Filosofova, "Basification of Plagiogneises at the Contact with Gabbroids of the Yurchik Massif in the Ganal Ridge, Kamchatka," Tikhookean. Geol. **21** (1), 29–47 (2002). 1

38. A. I. Khanchuk, "Geological Setting of the Granulite-Facies Rocks and Gabbronorites of the Ganal Ridge (Eastern Kamchatka)", Geol. Geofiz., No. 8, 45–51 1
(1978).

39. N. V. Tsukanov, *Tectonic Evolution of Pre-Oceanic Zone of Kamchatka in the Late Mesozoic–Early Cenozoic* (Nauka, Moscow, 1991) [in Russian].

40. V. I. Shul'diner, S. V. Vysotsky, and A. I. Khanchuk, "Crystalline Basement of Kamchatka: Structure and Evolution," Geotektonika **14** (2), 80–93 (1979).

41. S. A. Shcheka, "Gabbroid-Related Hornfelses and Granulite Rocks of Kamchatka," in *Petrology and Geochemistry of Magmatic and Metamorphic Rocks of the Far East*, Ed. by S. A. Korenbaum (Dal'nevost. Nauchn. Tsentr Akad. Nauk SSSR, Vladivostok, 1975), pp. 167–196 [in Russian].

42. M. B. Epel'baum and M. V. Bogolepov, "Melting in Fluid-Silicate Systems and Modeling of Granitization

Processes," in *Sketches in Physical-Chemical Petrology (Magmatism, Metamorphism, Mantle)*, Ed. by V. A. Zharikov and V. V. Fed'kin (Nauka, Moscow, 1991), No. 16, pp. 6–15 [in Russian].

43. H. E. Huppert and R. S. Sparks, "The Generation of Granitic Magmas by Intrusion of Basalt into Continental Crust," J. Petrol. **29** (3), 599–624 (1988).
44. B. E. Leake, "Nomenclature of Amphiboles," Can. Mineral. **16** (4), 501–520 (1978).
45. M. M. Lebedev, I. A. Tararin, and E. A. Lagovskaya, "Metamorphic Zones of Kamchatka as an Example of the Metamorphic Assemblages of the Inner Part of the Pacific Belt," Tectonophysics **4** (4–6), 445–461 (1967).
46. D. H. Lindsley, "Pyroxene Thermometry," Am. Mineral. **68** (5/6), 477–493 (1983).
47. I. D. Ryabchikov and A. L. Boettcher, "Experimental Evidence at High Pressure for the Potassic Metasomatism in the Mantle of the Earth," Am. Mineral. **65** (9/10), 915–919 (1980).
48. M. Schneider and D. Eggler, "Fluids in Equilibrium with Peridotite Minerals: Implication for Mantle Metasomatism," Geochim. Cosmochim. Acta **50** (5), 711–724 (1986).
49. T. W. Sisson, K. Ratajeski, W. B. Hawkins, and A. F. Glazner, "Voluminous Granitic Magmas from Common Basaltic Sources," Contrib. Mineral. Petrol. **148** (6), 635–661 (2005).

Recommended for publishing by O.V. Avchenko

SPELL: 1. Geol